THESIS

QUANTIFYING CLIMATE CHANGE IMPACTS ON FUTURE WATER RESOURCES AND SALINITY TRANSPORT IN A HIGH SEMI-ARID WATERSHED USING THE APEX-MODFLOW-SALT MODEL

Submitted by

Jaya Vignesh Balakrishnan

Department of Civil and Environmental Engineering

In partial fulfillment of the requirements

For the Degree of Master of Science

Colorado State University

Fort Collins, Colorado

Spring 2023

Master's Committee:

Advisor: Ryan Bailey
Co-Advisor: Mazdak Arabi

Michael Ronayne

ABSTRACT

QUANTIFYING CLIMATE CHANGE IMPACTS ON FUTURE WATER RESOURCES AND SALINITY TRANSPORT IN A HIGH SEMI-ARID WATERSHED USING THE APEX-MODFLOW-SALT MODEL

High salinity mobilization and movement from salt laden deposits in semi-arid landscape poses threat to impairment of soil and water resources worldwide. Semi-arid regions in the world are expected to experience rising temperatures and lower precipitation, which will impact water supply and likely spatio-temporal patterns of salinity loads affecting downstream water quality. No studies have evaluated salt fate and transport from high desert landscapes under the influence of future climate uncertainties. This study quantifies the impact of future climate change on hydrology and salinity transport and their total watershed yield in the Gunnison River Watershed (GRW) (14,608 km^2), Colorado, using the APEX-MODFLOW-Salt hydro-chemical watershed model and three different CMIP5 climate models output downscaled by Multivariate Adaptive Constructed Analogs (MACA), each for two climate scenarios, RCP4.5, and RCP8.5, for the period 2020–2099. The APEX-MODFLOW-Salt model accounts for transport of hydrology and major salt ions (SO_4^{2-}, Cl^-, CO_3^{2-}, HCO_3^-, Ca^{2+}, Na^+, Mg^{2+}, and K^+) to in-stream loading via various hydrological pathways (surface runoff, rainfall erosional runoff, soil lateral flow, quick return flow and groundwater discharge to streams). Results indicate that varying trends in precipitation output from different climate models with different RCP yields varying trends in annual average water yield (mm/ year) with predicted maximum and minimum change of +7.3% and -13.4% but annual average salinity loads (kg/year) discharged via watershed outlet simulation increased consistently with maximum and minimum change of +9.6% and +4.1% from the baseline scenario of 2007-

2017. From the results, this conjunction of APEX-MODFLOW-Salt model with downscaled future climate forcings can be a helpful modeling framework for investigating hydrology and salt mobilization, transport, and export in both historical and predictive settings for salt-affected watersheds in the world.

ACKNOWLEDGEMENTS

I would like to extend this opportunity to express my deep sincere gratitude and appreciation to my advisor, Dr. Ryan T Bailey for the great mentorship, kind, supportive and opportunities for growth provided to me. I am forever grateful to Dr. Ryan Bailey and Dr. Mazdak Arabi for taking a chance on me as graduate assistant with my minimal background. I consider myself extremely lucky and honor to work and study under their guidance which was invaluable and instrumental to shaping my engineering career. Special thanks to fellow graduate students and other researchers for assistance in completing components of research, including Cibi Chinnasamy, Elizabeth Motter, Zaichen Xiang, and Seonggyu Park. Thanks to all the professors who had me as a student in their fascinating coursework's in my graduate career, special thanks to Dr. Neil Grigg, for being my graduate advisor at initial stages of the graduate school and Dr. Michael Ronayne for agreeing to be on my research committee. This research was made possible with the funding from the United States Department of Interior – Bureau of Land Management. My time at Colorado State University and its community have given me enough experiences and knowledge to treasure for the rest of my life. Most importantly, I would like to acknowledge the tremendous support of my family members for their unwavering faith and love, without their encouragement the completion of this graduate school would not have been possible. Thanks to my friends.

TABLE OF CONTENTS

LIST OF TABLES

LIST OF FIGURES

1.INTRODUCTION

1.1 Salinity Mobilization and Transport in Watersheds

High salinity in soil water, groundwater and surface water causes impairment of soil and water resources worldwide. Salinization poses serious threats to food production, soil health, ecosystem biodiversity, municipal and industrial use of water and has become one of the most pressing issues for water quality globally (Vengosh, 2014; Zaman et al., 2018). Approximately 10% of arable lands in over 100 countries are affected by salinity and sodicity (Vengosh, 2014; Zaman et al., 2018) affecting mainly soil fertility and agricultural production (Hassani et al., 2020; Ivushkin et al., 2019). Salt afflicted regions are predominantly found in arid and semi-arid regions, for example in the western United States, eastern Australia, Mexico, the Middle East, China, Mongolia, and north and east Africa (Abbas et al., 2013; Ivushkin et al., 2019).

Salt mobilization and transport of salt mass to water sources occurs by both natural and anthropogenic means, with the first being primary driven by the dissolution of soluble salts (e.g., gypsum $CaSO_4$, calcite $CaCO_3$, sodium chloride NaCl) from soil and geologic units (Hassani et al., 2020; W. D. Williams, 1999) in areas with shallow groundwater that is in connection with channels, streams, lakes, and reservoirs (Hassani et al., 2020; Hosseini & Bailey, 2022). Anthropogenic influences include irrigation, vegetation clearing, mining activities, the use of road salt for deicing (Cañedo-Argüelles et al., 2013; Dugan et al., 2017), and effluent from wastewater treatment plants. Overall, the impact of salt on crop yield results in agricultural productivity losses of $10 billion per year (Ghassemi et al., 1995). Salt mass in watershed systems can be transported to nearby lakes, reservoir, and streams via surface runoff, rainfall erosional runoff, soil lateral flow, and groundwater discharge. In the Upper Colorado River

Basin (UCRB), a snowmelt spring-runoff semi-arid watershed with high salt loads in the river system, more than half of the total salt loaded in the river network originates from natural, non-irrigated rangelands (Miller et al., 2017; Bureau of Reclamation, 2013), costing upwards of approximately $300 million in economic damages (Bureau of Reclamation, 2013). The vast majority of salt mass is composed of eight major salt ions: SO_4^{2-}, Cl^-, CO_3^{2-}, HCO_3^-, Ca^{2+}, Na^+, Mg^{2+}, and K^+, which are products of salt mineral dissolution and applied fertilizer.

1.2 Studies Quantifying Salt Loading in Watersheds

Relatively few studies have investigated the significance of natural salinity loadings from high desert landscapes. Nauman et al. (2019) used a statistical modeling approach, random forest regression in conjunction with 30-m resolution maps of soil property and cover maps, to develop relationships between landscape features and annual in-stream salinity loading in the UCRB. This method used salt as a single constituent, not accounting for precipitation-dissolution chemical reactions of individual soluble salt ions present in salt minerals.

As studies (Nauman et al., 2019; Rumsey et al., 2017) indicate that groundwater is a significant source of salt to river systems in semi-arid regions, Bailey et al. (2022) linked the watershed model APEX (J. R. Williams & Izaurralde, 2010) with the groundwater flow model MODFLOW (Niswonger et al., 2011) and the groundwater solute transport model RT3D (Bailey et al., 2022; Clement, 1999) for salinity transport modeling in natural, high-desert landscapes. The authors developed a salt ion transport module for APEX, for the eight major ions, and a similar salt ion transport module for RT3D. The model therefore accounted for salt ion mass in soil water, groundwater, and stream water, with salt mass transported from the landscape to streams via surface runoff, erosional runoff, soil lateral flow, and groundwater discharge, subject to precipitation-dissolution reactions in soils and the aquifer. An initial application to the Price

River Watershed in Utah, USA, indicated that 88% of salt mass in the river system was derived from the aquifer via groundwater discharge. Other modeling efforts include (Tuteja et al., 2003) using a combination of CATSALT (salt mobilization and washoff) with 2D soil water flow and salt transport and 1D groundwater flow in southeastern Australia; and (Tirabadi et al., 2021) using a modified version of SWAT to simulate lumped salt transport in southern Iran.

1.3 Assessing the impact of Climate Change on Salt Loading

As per reports by the Intergovernmental Panel on Climate Change (IPCC), major arid and semi-arid regions are predicted to experience higher temperatures, lower rainfall, and reduced snowmelt (Hoegh-Guldberg et al., 2018; McCarthy et al., 2001; Ragab & Prudhomme, 2002). These changes in climate could have acute effects on salt pollution and transport in semi-arid regions, as soil salinity and groundwater salinity may increase and, through the process of groundwater salt loading to streams, cause increased downstream salinity.

Several studies have investigated the effect of climate change and future climate scenarios on salinity in watersheds. Schofield & Kirkby (2003) used spatial modeling within GIS to develop salinity indicators (low relief, two-way moisture flux, local flow deficit) and estimate their values in a future (2079-2099) climate represented by Global Climate Models. Olson (2019) used empirical models to estimate the effects of future land development (agricultural, industrial, and urban) and climate change on salinity in major streams and rivers of the United States. Corwin (2021) used three decades of remote sensing imagery to assess salinity development in soils, with a focus on arid, semi-arid, and coastal regions. More recently, Henson & Bailey (2023) used a version of the SWAT model (Arnold et al., 1998) with a salt transport module (Bailey et al., 2019) to assess the impact of change in future climate pattern with regards to salt loadings in the semi-arid Purgatoire River Watershed in southern Colorado, by applying 5% and

35% increases in storm intensity for a historical period. The scenarios of increased storm intensity resulted in 12% and 73% increase, respectively, in total salt mass export from the basin to the stream, with 99% of salt in the river sourced from subsurface water. However, the comprehensive analysis of the effects of future climate change on salt transport in semi-arid high-desert watersheds has not yet been undertaken.

1.4 Summary of Objectives

The objective of this study is to quantify the impact of future climate change on the mobilization, movement and loading of salt ion mass in a high-desert watershed for the 21st century. This study applies APEX-MODFLOW-Salt, a hydro-chemical watershed model, to the Gunnison River Watershed (GRW) (14,608 km^2), one of the eight 4-digit hydrologic unit watersheds in the Upper Colorado River Basin. This modeling approach simulates major hydrological processes and fluxes and associated salt ion chemical processes and loads, in surface runoff, rainfall erosional runoff, soil lateral flow, quick return flow, percolation from the soil profile to the aquifer, and groundwater exchange with streams. The model is tested against available measured streamflow and in-stream salt ion loadings, with the latter estimated using the LOADEST (Runkel et al., 2004) regression tool. This tested baseline scenario model is then used in conjunction with statistically selected Global Climate Models (GCMs) for various emission scenario's output for assessing relative changes of hydrologic fluxes and salt loads throughout the 21st century as compared to historical values.

2. METHODS

2.1 Study Region: Gunnison River Watershed, Colorado

The Gunnison River is the largest tributary to the Colorado River in Colorado, almost the volume of the Colorado River doubles after the Gunnison River convergence. The GRW, Colorado is one of 8 HUC 4 subbasins in the Upper Colorado River Basin (UCRB), rests on the west side of the Continental Divide, (latitude 37°51'- 39°15' N, longitude 106°13'-108°8' W) is shown in Figure 1A. The UCRB has a spatial area of approximately 294,000 km^2 covering the portions of Wyoming, Colorado, Utah, Arizona and New Mexico (Rumsey et al., 2017). It encompasses a wide range of lithology, topography, climate, and land cover types and uses. Salinity has always been a problem with the basin's water quality due to the nature of saline soils and geologic units in the basin (Anning et al., 2007; Mueller & Osen, 1988; Spahr et al., 2000)**,** costing estimated $300 to $400 million in economic damages annually (Reclamation, 2013).

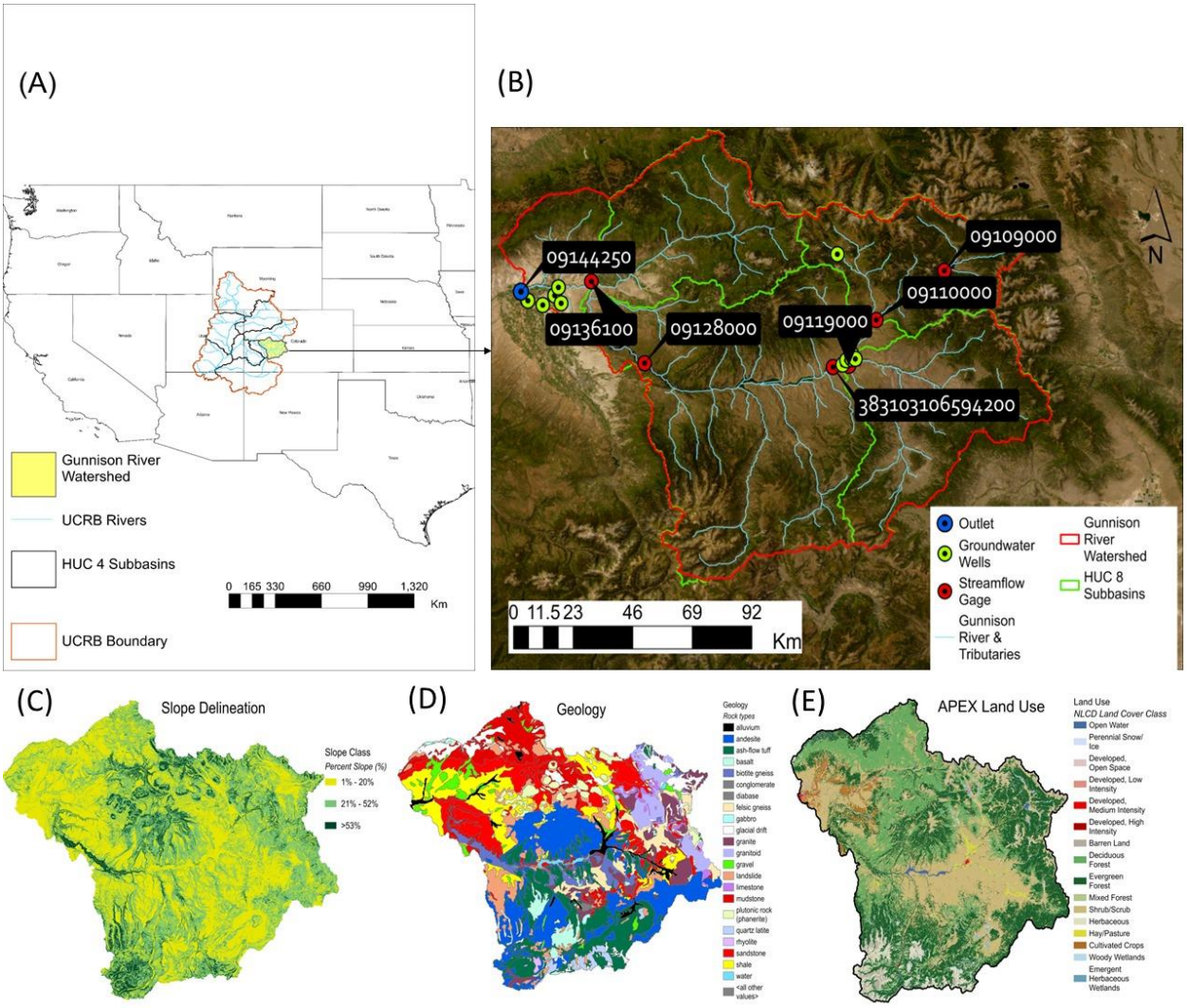

Figure 1- (A) Geographic and spatial extent of Gunnison Boundary representing its rivers, and HUC 4 subbasin's; (B) Map of Gunnison River Watershed (GRW) featuring its outlet, GW wells, Streamflow gage's along with its rivers and tributaries; (C) Slope percentage of GRW;(D) GRW Geology; and (E) GRW Land use from NLCD 2019.

The GRW study region comprises 4 out of 60 8-digit watersheds in the UCRB, namely East Taylor, Tomichi, Upper Gunnison, North Fork Gunnison, and parts of Lower Gunnison watershed subbasin. The GRW comprises the drainage area of 14608 km^2, covering entire Gunnison County and parts of Delta, Hinsdale and Saguache Counties, Colorado. The Headwaters of Gunnison River originate from confluence of the Taylor and East rivers at Almont in eastern Gunnison. The Gunnison River flows ~190 km from Almont to the Outlet Confluence Park, Delta, CO in Delta County. While the GRW is situated in the semi-arid western part of the United States,

the main hydrological process is governed by snowmelt spring runoff during late spring and early summer from mountainous highland areas and in low elevations, most of the precipitation falls as rain in late summer and early fall. In general, the temperature is warmer relative to the high elevation. The Aspinall unit in this mountainous watershed in the upper part of the Black Canyon features three dams namely Blue Mesa Dam, Morrow Point Dam and Crystal Dam built as in the part of the Colorado River Storage Project which primarily regulates flow along the western part of the basin implemented by the Bureau of Reclamation for irrigation diversion to Uncompahgre River through Gunnison tunnel serving over 76,000 acres of project land, municipal use, regulation of water rights, flood control, recreational activities and hydroelectric power generation. Since all the tributaries joining the Gunnison is mainly driven by snowmelt are ephemeral which have carved a complex network of canyons and mesas through the basin during high summer flows. The basin receives an average rainfall of 280mm/year and an average snowfall of 1219mm/year, with average monthly temperatures ranging from -10°C (January) to 16.7°C (July).

A defining characteristic of this watershed is the steep slope gradients, with an average slope of 25% and maximum slope of 87% (the Black canyon Gorge) are shown in Figure 1C. The elevation ranges from 4,363 m in the Sheep Mountain & Uncompahgre Peak to 1,499 m in Confluence Park, Delta. The GRW is mainly composed of low-lying irrigated cultivation along the river and tributary corridors, high desert shrubland, and forested mountain areas as shown in Figure 1E. As per NLCD 2019 (CONUS), The predominant land uses are evergreen forest, shrubland and deciduous forest covering 34%, 32% and 19% of the basin, respectively. The National Land Cover Database (NLCD) classifies less than 1.1% of the basin as developed. The mountains in basin are vegetated with evergreen and deciduous forest along the steeps and found sparsely throughout the rangeland. A large percentage of land in the study area is owned and

managed by the U.S Forest Service followed by Bureau of Land Management and private owners. The geologic units that are predominantly found in the upper part high elevations areas of the watershed include andesite, gneiss, granite, and ash-flow tuff whereas the lower part lower elevation regions include sandstone, shale and mudstone, with slope-wash deposits and alluvium (clay, silt, sand, granules, pebbles and cobbles) along the drainage areas of the Gunnison River stream system. Studies have indicated that the saline soils and geologic units in the UCRB are natural source of salinity within the watershed (Anning et al., 2007; Mueller & Osen, 1988; Spahr et al., 2000)**.** The GRW Soil maps of Calcium Carbonate ($CaCO_3$) and Gypsum ($CaSO_4$) is featured in Figure 5.

Streamflow patterns in the GRW are dominated by spring snowmelt processes (Figure 2). However, in lower elevation of the watershed, despite the late spring and early summer snowmelt, a small increase in streamflow can be observed as result of summer thunderstorms between July and August. Figure 2 is set up by averaging monthly available period of streamflow across months, therefore hydrograph fluctuations due to summer thunderstorms are not depicted. At a reservoir downstream (USGS 09109000 & USGS 09128000) (see Figure 1B), the streamflow pattern during early fall (late August to mid-September) differs from other sites snowmelt hydrograph due to controlled release of water to the stream.

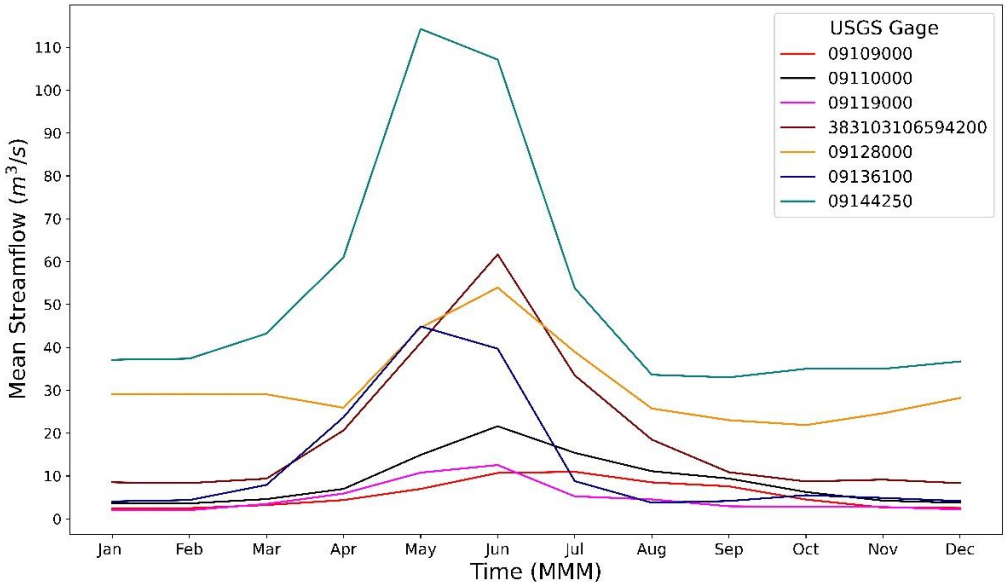

Figure 2- The Gunnison River Watershed's mean streamflow (m3/s) at different USGS stream gage site.

Field water-quality samples were obtained from the USGS at streamflow sites to study the loading of salt ions within the river system. There are a total of 2280 concentration measurements at the streamflow sites. Table 1 shows a summary of average annual streamflow and estimated salt ion loads using available concentration data, indicating the large influence of Ca and SO_4 on total salt loads. Results show the salinity increases with distance downstream, as salt is loaded via tributaries and groundwater. These streamflow and field measurements are used in this study in conjunction with LOADEST to estimate monthly in-stream salt ion loads (see Section 2.2.2). Measured salt ion concentrations in groundwater were obtained from USGS monitoring wells (see Figure 1B). There are a total of 227 measurements for 13 wells.

Table 1- The Salt Constituent information obtained by sampling for water quality analysis at USGS stream sites within the study region.

USGS Site Number	Site Name	Site Description	Average Annual Streamflow (m^3/s)	Average Instream Salt Constituent load (kg/day)	Average Salt Constituent (%)		Average Salt Concentration (mg/L)	
					SO_4	Ca	SO_4	Ca
09109000	Taylor River below Taylor Park Reservoir, CO	Taylor Dam Outlet	5.6					
09110000	Taylor River at Almont, CO	East Taylor Outlet	8.8					
09119000	Tomichi Creek at Gunnison, CO	Tomichi Outlet	4.8	37000	23	45	17.2	35
383103106594200	Gunnison River At CNTY RD 32 Below Gunnison, CO	Blue Mesa Reservoir Upstream	20	140000	27	52	15.4	30.6
09128000	Gunnison River Below Gunnison Tunnel, CO	Blue Mesa Reservoir Downstream	31	226000	32	44	17	24
09136100	North FK Gunnison River above mouth NR Lazear, CO	North Fork Outlet	13	289000	59	33	321	99
09144250	Gunnison River at Delta, CO	Gunnison Outlet	52.3	948000	60	20	195	65

2.2 Simulating Salinity Transport using the APEX-MODFLOW-Salt model:

This section describes the use of the APEX-MODFLOW-Salt watershed model to simulate the reactive transport of salt ions within the GRW. We will first describe the base hydrologic model, APEX-MODFLOW, and then present the modification of this model to include salt ion transport in the watershed system.

2.2.1 Simulating Hydrological Processes using APEX-MODFLOW

APEX-MODFLOW theory

The watershed model APEX is distributed, continuous, daily time-step model competent in simulating hydrological and water quality processes at field level to watershed scale with respect to 12 major components such as climate, hydrology, crop growth, pesticide fate, nutrient cycling, erosion-sedimentation, carbon cycling, management practices, soil temperature, economic budgets, and subarea/watershed routing. The APEX divides the watershed into subareas based on relative homogeneity of soil, weather, land use, and management practices. The model's routing mechanism allows for the study of interactions between subarea landscapes involving simulated surface runoff, erosion runoff, return flow, sediment deposition and degradation, transfer of nutrients and pesticides, and groundwater flow to subarea streams which are connected upstream to downstream for the watershed. The APEX modeling code is written in FORTRAN and available publicly.

Since the groundwater routines in APEX are simpler in treating hydrogeologic processes in a lumped, steady-state manner, the groundwater flow model MODFLOW has been linked to APEX as a single modeling code to simulate physically based spatially distributed groundwater modeling to provide groundwater head, recharge, and groundwater-surface water interactions. The description of this linked model and several preliminary applications to watersheds are provided in (Bailey et al., 2021). The MODFLOW groundwater model is a three-dimensional, physical based, distributed, finite difference groundwater model that solves the groundwater conservation of mass equations in the set of grids according to aquifer physical properties and available groundwater head to simulate the flow through aquifers providing groundwater recharge, evapotranspiration, pumping, and discharge to subsurface drains and surface water

features. MODFLOW is developed by USGS and written in the FORTRAN code and is free public domain software.

The loose coupling between APEX and MODFLOW was introduced by (Bailey et al., 2021). A further modification to the code to include reactive solute transport via RT3D was introduced by Bailey et al. (2022) and is presented in Section 2.2.2. Figure 3 shows the cross-section of a typical watershed setting representing processes simulated by APEX and MODFLOW/ RT3D, respectively. The APEX routine simulates hydrologic processes such as surface runoff, ET, plant growth, soil lateral flow, quick return flow, and deep percolation to the water table, whereas hydrogeological processes simulated by MODFLOW routines are groundwater storage, groundwater head, and groundwater-surface water interactions. The return of groundwater flow to subarea streams depends on the stream stage with respect to the aquifer head since the groundwater flows from higher potential to lower potential the stream can be either gaining or losing the water. Figure 3 indicates a gaining stream condition. Upon running the integrated model APEX-MODFLOW, loose coupling occurs as APEX simulates subarea landscape processes passes soil percolation (also known as recharge) from each subarea to the group of MODFLOW grid cells that are located inside the subarea geographic boundaries. Grid cells are geographically connected to subareas using Geographic Information System (GIS) intersection techniques. Using these recharges as sources along with grid cells values of hydraulic conductivity, specific yield, and specific storage, the MODFLOW simulates new groundwater storage and groundwater head for each grid cell. The resulting groundwater heads are used to compute groundwater-surface water interaction between MODFLOW river grid cells and APEX subarea streams that intersect, using Darcy's law. More details are provided in (Bailey et al., 2021). This coupling between APEX subareas and MODFLOW grid cells

simulation occurs on a daily time step. To provide a single FORTRAN code and executable, MODFLOW subroutines and essential linking subroutines are embedded inside the APEX modeling code. The integrated APEX-MODFLOW model was applied previously to the Animas River Watershed (Colorado, New Mexico; 3,542 km2), the Price River Watershed (Utah; 4,886 km2), and the Middle Bosque River Watershed (Texas, 470 km2) to assess streamflow and groundwater head (Bailey et al., 2021).

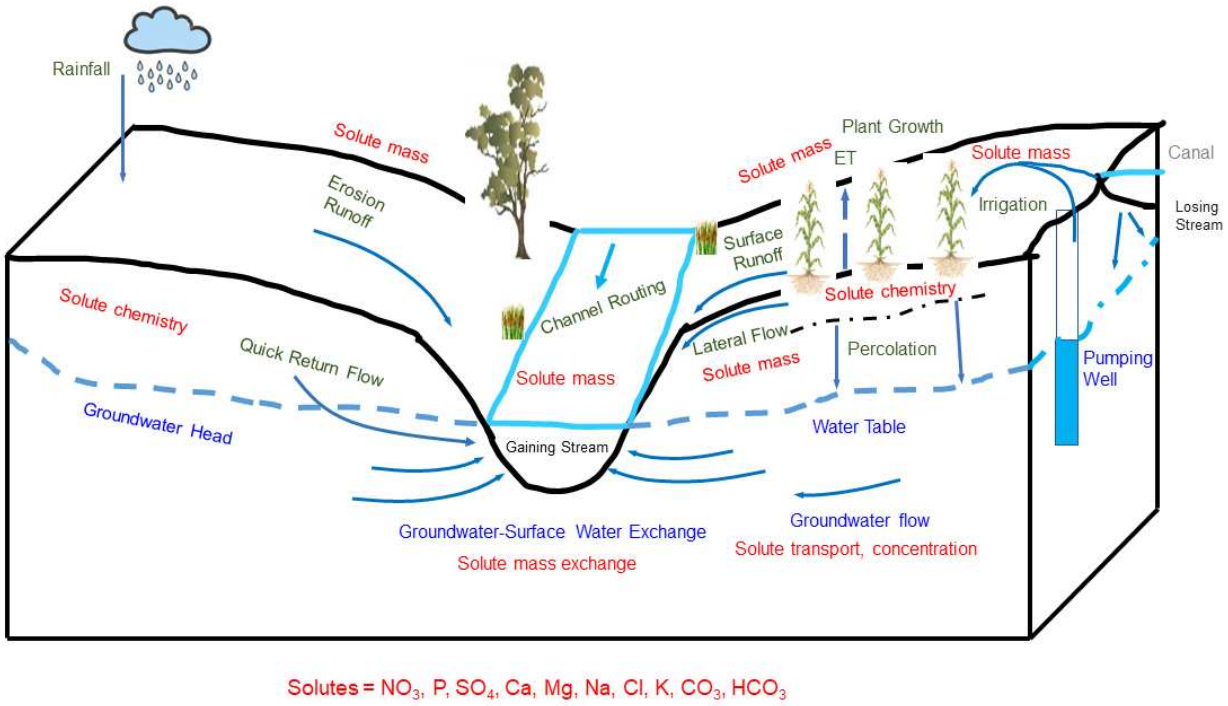

Figure 3- The Representation of typical watershed system's cross section, green text depicts the hydrological processes simulated by APEX model, blue text shows the subsurface hydrological processes simulated by MODFLOW grids, and red text shows the simulation of salinity fate and transport processes by APEX and RT3D model.

APEX-MODFLOW model for the Gunnison River watershed

The APEX-MODFLOW model was constructed and calibrated by colleagues at Texas A&M University. The APEX model construction for the GRW follows the same procedures as for the other watersheds presented in (Bailey et al., 2021). The APEX model input files were created in the ArcAPEX environment, a plugin tool within ArcMap. Using 30 m National

Elevation Dataset (https://apps.nationalmap.gov/downloader/), the landscape of the study watershed is divided into 219 subareas, ranging from 0.007 km^2 to 343.5 km^2 and averaging 66.64 km^2. These subareas, land cover and soil type are used to represent and simulate watershed hydrology which were assigned based on unique combinations of slope, land use and soil type. Daily precipitation, maximum and minimum temperature, obtained from NOAA- National Climate Data Center, as described in (White et al., 2017; Worqlul et al., 2021) weather variables are key factors in influencing and simulating the surface runoff in watershed APEX model based on modified NRCS curve number method. The curve number retention parameter S requires continuous soil moisture accounting procedure. The simulated daily runoff in subareas is routed to their channels downstream using the variable storage coefficient flood routing method, Figure 4 represents the model subareas with river channel**.** Since snowmelt is the primary driver of hydrological process in the GRW, APEX simulates snowmelt based on the empirical relationship between air temperature and melting rates as described in (Hock, 2003). The Potential daily evapotranspiration rates in APEX were estimated by selecting the Hargreaves method (Hargreaves & Samani, 1985) that requires only daily maximum and minimum temperatures.

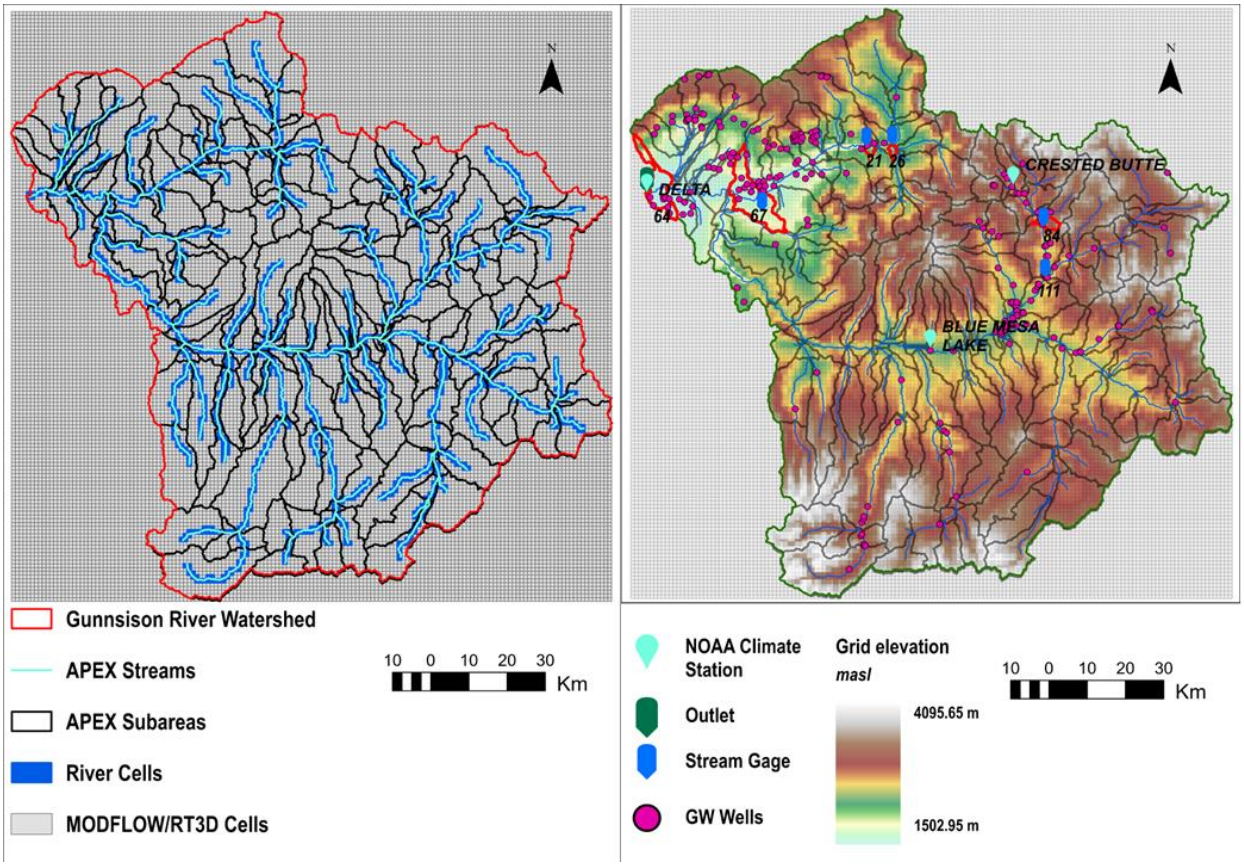

Figure 4- Displaying the map of GRW delineated APEX Subareas, Streams, River Cells, MODFLOW/RT3D Grid cells with colored grid elevation within GRW boundary, along with selected Stream Gage sites for calibration, selected NOAA climate station for GCM statistical evaluation, Groundwater wells and Outlet gage.

The MODFLOW grid is constructed based on spatial extent of APEX model watershed landscape. The number of MODLFOW rows and MODFLOW columns for the GRW are presented in Table 2. The total number of MODFLOW grid cells for the GRW model are 24,649, where each squared cell side is 1,000 m with cell area of 1 km^2. The inputs included for MODFLOW model each grid cells are hydraulic conductivity(m/day) based on Gunnison surface geology, ground surface elevation (m) from digital elevation model and aquifer thickness (m). The Initial hydraulic conductivity (m/day) and specific yield for the Gunnison MODFLOW model grid cells were computed based on the permeability maps of (Huscroft et al., 2018) (https://borealisdata.ca/dataset.xhtml?persistentId=doi:10.5683/SP2/TTJNIU) for unconsolidated near surface units. The Ground surface elevation (m) for model each grid cells was resolved from

30 m National Elevation Dataset (https://apps.nationalmap.gov/downloader/). The aquifer thickness, i.e., the depth to bedrock (m) for each grid cells was resolved from the 250-m resolution aquifer thickness map of (Shangguan et al., 2017) (http://globalchange.bnu.edu.cn/research/dtb.jsp). The unconfined aquifer is represented using a single layer of grid in MODFLOW model. Figure 5 shows the map of some basic model inputs given to the study watershed APEX-MODFLOW model.

Table 2- The features of watershed system and APEX-MODFLOW model for the GUNNISON River Watershed

Feature	**Gunnison River**
State	CO
Size (km^2)	14608
Climate	Semi-Arid
Elevation (m)	1499-4363
Avg. Rainfall (mm/year)	280
Avg. Snowfall (mm/year)	1219
Temperature (°C)	-10 – 16.67
APEX Subareas	219
MODFLOW Rows	157
MODFLOW Columns	157
MODFLOW Cell Size(m)	1000
MODFLOW active cells	19,917
MODFLOW River Cells	1943
Simulation Period	2007-2017

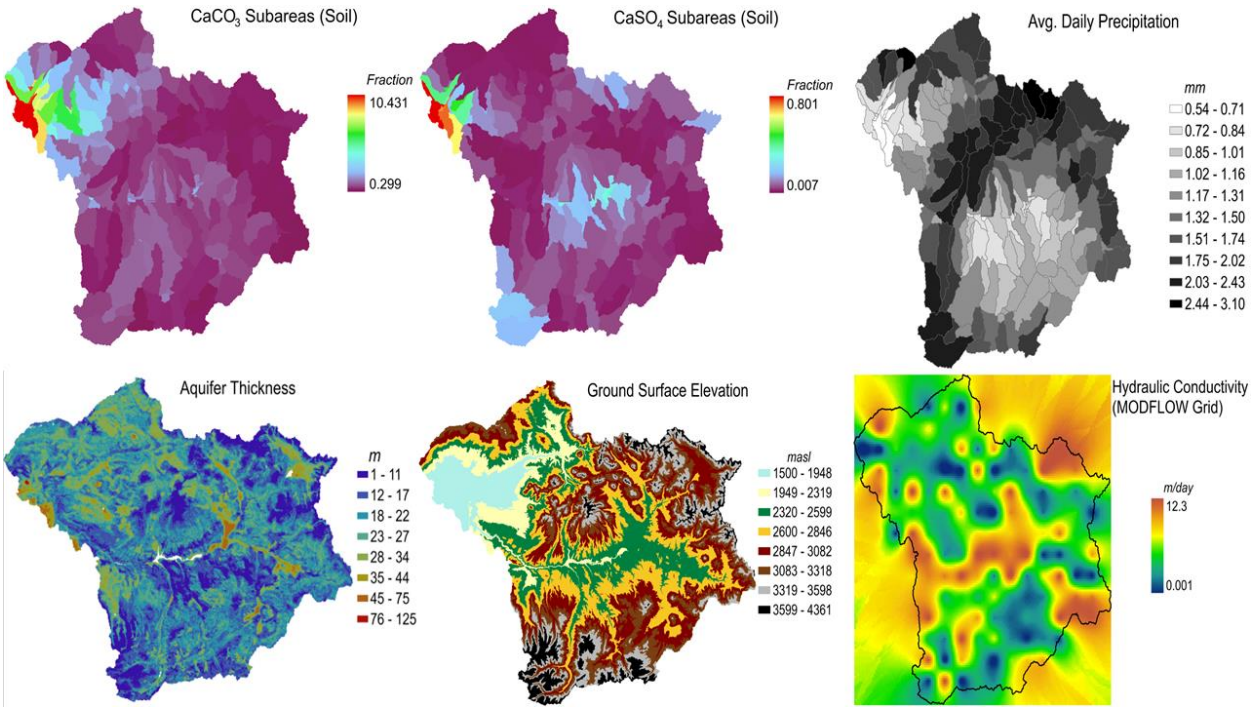

Figure 5- The basic APEX model inputs for the Gunnison River Watershed are shown as maps in first row for Salt mineral in soil fractions CaCO3, CaSO4, and precipitation. The basic MODFLOW/RT3D inputs representing model aquifer system are portrayed as maps for Aquifer thickness, Ground surface elevation and Hydraulic conductivity in second row.

Further, the constructed APEX and MODFLOW model of the GRW was linked according to the linkage details provided above and detailed in (Bailey et al., 2021). After linkage, the number of active grid cells used for simulating the groundwater routine in MODFLOW grid cells within the watershed boundary is 19,917. The number of river grid cells used for exchanging groundwater and surface water rates along the subarea streams are 2,194. The features of watershed system and information on the APEX-MODFLOW model are presented in Table 2. The colored grid cells featuring land surface elevation (m) are coupled with delineated subarea for the GRW are shown in Figure 4, with APEX river network and associated river grid cells. The GRW elevation ranges from the mountains to lower plain areas. This coupled APEX-MODFLOW is simulated for periods between 2007 and 2017 for 11 years.

APEX-MODFLOW model calibration

The simulated APEX-MODFLOW model was tested against the measured streamflow (monthly) and groundwater head from stream gage sites and monitoring wells maintained by the USGS. Due to limited availability of data, in our study region the GRW, the six stream gage stations (Figure 4) recording streamflow discharge values for monthly scale varying length of record where except one gage station all others had streamflow record from 2012 to 2017, which had period of record from 03/2015 to 2017 (one among the other 5 gage sites is located at outlet of the watershed) and one groundwater monitoring well site (USGS 384306108013801) where daily measured GW head available from March 2015 to March 2017 were used for calibration process. Since the entire model was simulated for 11 years from January 1,2007 to December 31, 2017, the first five years of model simulation were considered as warmup period (1/1/2007-12/31/2011). The remaining period of simulation (1/1/2012- 12/31/2017) where six years were considered for model calibration.

The APEX-MODFLOW hydrologic and hydrogeologic parameters were estimated using the automatic model calibration program PEST (Parameter Estimation) (Doherty, 2018), an independent parameter estimation and uncertainty analysis model that can be coupled with any environmental numerical modelling software. The optimization algorithm used in PEST for estimating model parameters is the Gauss-Levenberg-Marquardt algorithm. This search algorithm iteratively changes values of specified model parameters to minimize the sum of the squared weighted residuals between the observed data and simulation values:

$$\Phi = \sum_i^n w_i(o_i - s_i)^2 \qquad \textit{(Equation 1)}$$

where Φ is the objective function, n is the number of measured data, w_i is the weight assigned to the i^{th} target measured data, and o_i and s_i are the measured and simulated values of the i^{th} target

data, respectively. The value of weight w_i for each specified target variable is calculated as the product of an uncertainty weight and a unit discrepancy weight. The value of an uncertainty weight was determined as the inverse of an estimated coefficient of variation reflective of the relative uncertainty in the observations of the target variable. The value of a unit discrepancy weight was computed by unifying the sum of the square of each observed variable value. The PEST requires three types of input files called template files, instruction files and control files, as detailed in (Park, 2018) to execute parameter estimation iteration. This type of modeling framework which uses PEST to calibrate the coupled surface/subsurface hydrologic model was first introduced by (Park, 2018)**,** further modified in the study (Liu et al., 2020) to include the distributed, parallel implementation of PEST called BEOPEST as the PEST-executable file to considerably shorten the calibration time is adopted for this study. More detailed information about the optimization process and principles of PEST can be found in (Zhulu, 2010) and the PEST manual (Doherty, 2018).

Both APEX and MODFLOW parameters required to be automatically calibrated were grouped together in PEST control file along with other required information to get started the estimation iteration. The APEX parameters included for the calibration procedure are provided in Appendix A Table 7. The MODFLOW parameters included were aquifer hydraulic conductivity, and aquifer specific yield, where grid values of these parameters were grouped together by pilot points as a set of spatially distributed parameters in the upper layer of the grid (only one layer of unconfined aquifer is used). These pilot points are passed to the MODFLOW model grid as an input array for hydraulic conductivity and specific yield using geostatistical approach, which is spatially weighted combination of pilot point values, following the guidelines in (Doherty et al., 2011).

2.2.2 Simulating Salt Ion Transport using APEX-MODFLOW-Salt

APEX-MODFLOW-Salt theory

The APEX-MODFLOW model of (Bailey et al., 2021) was modified to include salt ion storage and transport in the watershed system by (Bailey et al., 2022). This was accomplished by (1) implementing a new salt ion transport module into the APEX subroutines for land surface, soil, and channel systems, and (2) including the groundwater reactive transport model RT3D into the MODFLOW subroutines, with salinity equilibrium chemistry functionality for salt ions. The APEX-MODFLOW-Salt model therefore simulates the fate and reactive transport of eight major ions (SO_4^{2-}, Cl^-, CO_3^{2-}, HCO_3^-, Ca^{2+}, Na^+, Mg^{2+}, K^+) in soils, aquifers, and streams of a complex watershed system. Salt loading to streams occurs via surface runoff, erosion runoff, soil lateral flow, and groundwater discharge.

The salinity fluxes transported via surface runoff, soil lateral flow, and streamflow are simulated in APEX in the same manner as nitrate (NO_3^-) except for erosion runoff. The salinity chemistry simulation in APEX is based on Salinity Equilibrium Chemistry (SEC) module (Shapiro & Shapley., 1965; Tavakoli-Kivi et al., 2019) developed for soil and aquifer systems. The equations used in other water chemistry models (e.g., UNSATCHEM:(Šimůnek et al., 2012); PHREEQC: (Parkhurst & Appelo, 2013) are used to describe the chemistry of salt ion solutions. These equations can be used to evaluate the dissolution of salt minerals in both soil and water. Using stoichiometric algorithm (Lindsay, 1979; Parkhurst & Appelo, 2013)**,** mass balance and mass action equations (Bailey et al., 2019; Lindsay, 1979; Shapiro & Shapley, 1965) are solved simultaneously to calculate the concentration of salt ions assists in ideal simulation of precipitation and dissolution of salt minerals. Based on the solubility of each mineral, precipitation is simulated when the ion content in the soil or aquifer layers is super-saturated, and

dissolution is simulated when the mineral content in the soil layer or aquifer is under-saturated. The five salt minerals and their dissolution that are included in APEX-MODFLOW-Salt include in the SEC module are $CaSO_4$, $CaCO_3$, $MgCO_3$, NaCl, and $MgSO_4$.

For erosion runoff, the polynomial regression equation is implemented to estimate the simulated concentration (mg/L) of total dissolved solids (TDS) in runoff water (Bailey et al., 2022). The following polynomial regression equation was developed based on research performed on hundreds of field samples collected during rainfall-runoff field tests in the desert shrublands of the UCRB by the BLM (Bureau of Land Management) (Colorado River Basin Report: BLM, 2015) was developed by (Kim et al., 2022). The APEX code incorporated equation for erosion runoff (Bailey et al., 2022):

$$TDS = 160256 - 1.246x_1 + 0.0901x_2^2 - 0.00031x_2^3 + 1.296x_3 - 17.44x_4 + 0.1557x_4^2 + 1.287x_5 - 60865x_6 + 7659x_6^2 - 319x_6^3 + 171x_7 - 14.03x_7^2 \quad \textit{(Equation 2)}$$

From equation 2, where TDS is in mg/L, x_1 = runoff during a rain event (mm); x_2 = sediment concentration (g/L); x_3 = rock fraction of the soil; x_4 = sodium adsorption ratio (SAR); x_5 = cation exchange capacity (CEC) (mg/L); x_6 = pH of the soil water; and x_7 = electrical conductivity (EC) of the soil water. APEX simulated runoff (mm) and sediment concentration (g/L) during a rainfall event. SAR and CEC equations are calculated based on the ion concentrations in the topsoil layer in the watershed (Bailey et al., 2022), whereas the watershed soil survey assumed constant are assigned to rock fraction, electrical conductivity, and pH of the soil water. After the TDS concentration during a rain event has been calculated, the concentration of each salt ion in the runoff is computed by taking the ratio of salt ion to TDS in the soil water of the topsoil layer. Just the same as salt ion mass in surface runoff and soil lateral flow, the salt ion mass simulated

from erosion runoff is transported to the subarea stream to carried through watershed river system.

The RT3D modeling code implemented in APEX-MODFLOW is called as subroutine after MODFLOW routines have finished on a daily time step. Using the groundwater head, cell by cell flow data, and groundwater sources/sink flow rates from MODFLOW, the RT3D model simulates reactive transport of solute in accordance with advection, dispersion, and chemical reactions. The conservation of mass advection-dispersion-reaction equation is used to track the mass of each solute is described in detail (Bailey et al., 2022)**.** The initial concentration of salt ion to RT3D code is passed from APEX subroutines, therefore concentration of salt ion in recharge water is based on salt minerals mass leached from subarea soil profile to RT3D grid cells. Similarly salt mass delivered via stream seepage is mass carried in subarea stream transferred form runoff, lateral flow, and leaching. However, in the end salt mass can be influx or efflux in the watershed river system based on both stages of stream and aquifer.

The code structure shown in Figure 6 describes how APEX original code for hydrology has been modified to include a subroutine for soil salt ion chemistry, followed by a call to other subroutines MODFLOW simulating hydrogeologic condition and RT3D simulating reactive transport of salt ions in the aquifer system.

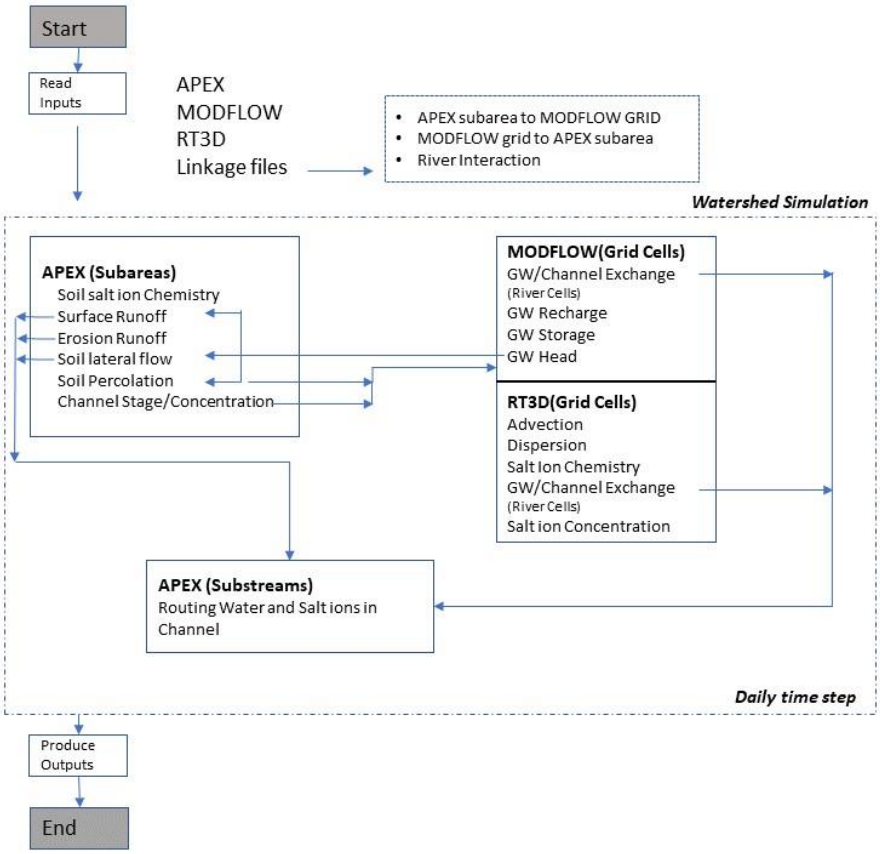

Figure 6- The Workflow structure of APEX-MODFLOW-Salt Modeling code.

The model code starts by reading and storing input variables from APEX files, MODLFOW files, RT3D files and linkage files, whereupon the watershed simulation is run using daily timesteps. The watershed simulation follows the original APEX modeling code for simulating land surface, subsurface hydrologic, and chemical simulations, with the modified subroutine for soil salt ion chemistry, followed by call to the MODFLOW subroutine and RT3D subroutine. After simulating subarea hydrology processes in APEX, linking subroutines are called that prepare APEX data (soil percolation, channel stage, soil percolation salt ion mass, in-channel salt ion concentration) to convert APEX subarea variables to MODFLOW grid variables and RT3D grid variables (APEX SI-Units to Grid units) for use by these Grid models. At end of MODFLOW and RT3D subroutine, Groundwater-surface water exchange rate, and

Groundwater-surface water salt ion exchange mass are transported to APEX Substreams (subarea channels) along with surface runoff, erosion runoff, and soil lateral flow Detailed information on the standard inputs and outputs for the APEX, Salinity module, MODFLOW subroutine and RT3D subroutine are provided in (Bailey et al., 2022)**.** The watershed routing in the model transports these added salt ion mass and water in the channel from one subarea to another subarea throughout the model domain till reaches the outlet. The simulated daily mass budgets of salt ion mass are tracked in surface runoff, soil lateral flow, erosion runoff, soil layers, precipitation-dissolution, soil leaching, groundwater discharge to streams, and stream seepage to groundwater.

Application of APEX-MODFLOW-Salt to the Gunnison River Watershed

After calibrating and testing the coupled APEX-MODFLOW model of the GRW for baseline hydrology is integrated with new salinity module and modified RT3D (uses same MODFLOW grid) modeling code for simulating salinity fate and transport in APEX soil water and groundwater aquifer system. Since more than half of the total salinity loads contributed to the UCRB is said to have originated from saline soils and geologic units that present under irrigated lands of watershed (Kenney et al., 2009; Miller et al., 2017) are regarded as natural sources of salinity in the watershed (Anning et al., 2007; Mueller & Osen, 1988; Spahr et al., 2000) due to soil erosion (Cadaret et al., 2016; Tillman et al., 2018; Tillman & Anning, 2014; Weltz et al., 2014) and dissolution processes (Rumsey et al., 2017). Therefore, the salt ion chemistry in APEX salinity module and RT3D reactive transport of salt ions are provided with Salinity Equilibrium Chemistry (SEC) module, primarily developed for soil and aquifer systems which updates salt ion concentrations according to stoichiometric algorithm.

To simulate salinity fate and transport within watershed, the developed SEC module should include five soil salt minerals ($CaSO_4$, $CaCO_3$, $MgCO_3$, NaCl, and $MgSO_4$) and eight salt ions (SO_4^{2-}, Cl^-, CO_3^{2-}, HCO_3^-, Ca^{2+}, Na^+, Mg^{2+}, and K^+) that dissolves from these minerals as an initial value to the model. The Salt minerals Gypsum ($CaSO_4$) and Calcium Carbonate ($CaCO_3$) for each subarea and each grid cell in the GRW model were zonal calculated for subarea and it's spatially joined for grid cells in the ArcGIS Pro based on the 30-m resolution predictive soil property maps for the Colorado River Basin above Lake Mead near surface geologic units from (Nauman & Duniway, 2020) (https://www.sciencebase.gov/catalog/item/5e063e5ce4b0b207aa0a6f45). Figure 5 depicts the map of $CaSO_4$, and $CaCO_3$ mineral fraction delineated by APEX subareas. Since no soil salt minerals data available for $MgCO_3$, NaCl, and $MgSO_4$, all subbasins and grid cells of soil and aquifer systems corresponding to the Gypsum and $CaCO_3$ content were given a small homogenous arbitrary value of mineral content of 0.25%, 0.3% and 0.05% for $MgCO_3$, $MgSO_4$, and NaCl respectively. The Ground Water initial salt ion concentration for all eight ions in soil water is collected form USGS National Water Information System Groundwater wells shown in Figure 4 (https://maps.waterdata.usgs.gov/mapper/index.html) in form of point data resolution are spatially interpolated using Radial Basis Functions (RBF) deterministic method, where this geostatistical analysis results are spatially joined for subareas and grid cells. These estimated initial values of soil salt minerals and soil water ion concentrations for each subarea and each grid cell were given as input to the model in files named *salt_input* for subareas and *rt_Gunnison.salt* and *rt_Gunnison.btn*. These values were manually adjusted during calibration step in trial-and-error approach until best matching spatial and temporal pattern is achieved between simulated and observed salt variables. The APEX salinity module reads in input initial

salt information from *salt_input* for salt minerals and salt ions in water whereas the RT3D modelling code reads information from *rt_Gunnison.salt* for salt minerals and *rt_Gunnison.btn* for salt ions in water. The datasets used in construction of APEX-MODFLOW-Salt model are similar in their spatial resolution and sources were used in (Bailey et al., 2022)**.**

APEX-MODFLOW-Salt model calibration and testing

In general, of corresponding days the instream salt loads simulated from APEX-MODFLOW-Salt model should be tested against measured salt ion load in streams at USGS gauge. However, the USGS gage measures only concentration of ions rather than salt ion loads. Due to the high cost of sample collection and processing, and frequent collection of salt ions concentration data is far less typical. Therefore, the USGS developed a FORTRAN program for estimating the constituent load in streams called LOAD ESTimator (LOADEST) by (Runkel et al., 2004). The software is freely available to public at (https://water.usgs.gov/software/loadest/). LOADEST estimates daily salt loads using available regression models supplied with any discharge values, available constituent concentration and additional data variables (calibration). This developed regression equations can be used to estimate loads for specified time interval using functions of streamflow and other additional specified data variables such as specific conductance (measured daily along with streamflow discharge) and decimal time as explanatory or predictor variables (estimation). Since three statistical estimation methods in LOADEST form the basis for calibration and estimation procedures by computing model coefficients for the regression model, of which adjusted maximum likelihood estimation (AMLE) is usually preferred, and it requires residuals of each ion to be normally distributed. More background information and software application guide are available at (LOADEST manual).

At the GRW outlet (Subarea 64), the USGS streamflow gage 09144250 Gunnison River at Delta, CO has measured 41 samples of HCO_3^-, 38 samples of Ca^{2+}, Mg^{2+}, Cl^-, Na^+, and K^+, and 12 samples of SO_4^{2-} over the period from 2009-2017. These measured samples of salt ion concentration were supplied to LOADEST along with historic daily corresponding discharge data (m^3/s) to account for daily salt load that could be delivered to stream for defined period was computed using AMLE method. This estimation method resulted residuals of each ion load were determined to be normally distributed. Figure 7 shows residuals are normally distributed for predicted salt ions load of Ca and SO_4. Since positive and negative residuals are scattered, without any trends says that model is independent and homoscedastic (having constant variance).

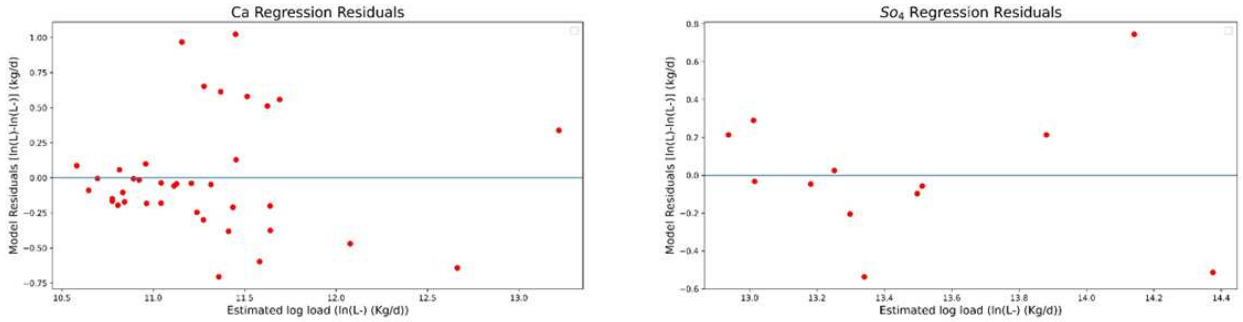

Figure 7: Represents residuals are normally distributed for predicted salt ions load of Ca and SO4

Table 3 displays the results of performance metrics that aids in comparing LOADEST results to measured values for each ion are the AMLE regression statistics, the load bias in percent (BP) and the Nash Sutcliffe Efficiency Index (NSE). Higher AMLE R^2 suggests better fit for the model. Positive BP values indicate over estimation, and negative BP values indicate underestimation. Also, warned by LOADEST that model estimation results should not be used when BP exceeds + or – 25%. NSE value near to 1 says perfect fit to observed data. The regression equation selected from LOADEST model to calculate the daily load estimate of each salt ion are provided in the APPENDIX B Table 8.

Table 3- Performance statistics from the LOADEST results for each of the 7 salt ions that had input data.

Salt Ion	AMLE R^2 (%)	BP (%)	NSE
HCO_3^{2-}	30.12	-6.65	0.45
Ca^{2+}	63.06	-2.77	0.74
Mg^{2+}	66.35	-0.12	0.76
Na^{+}	42.39	-5.11	0.38
Cl^{-}	0.48	52.23	-0.89
K^{+}	57.66	0.22	0.81
SO_4^{2-}	63.36	-3.27	0.47

Further, the LOADEST results are visually corroborated by plotting the estimated daily load of each salt ion against the available daily measured salt ion loads except for CO_3 (no measurements are available), which are calculated by multiplying the daily-averaged flow rate (m^3/day) by the discrete concentration measurement (g/m3) of each salt ion, assumed to represent the average value for the day. Figure 8 represents the graphs comparing daily salt load estimates against the measured salt ion load for the respective day. From Figure 8**,** we can say LAODEST estimates best for measured Ca, So_4 and Mg salt loadings and worst fit for Cl and other salt ion loadings.

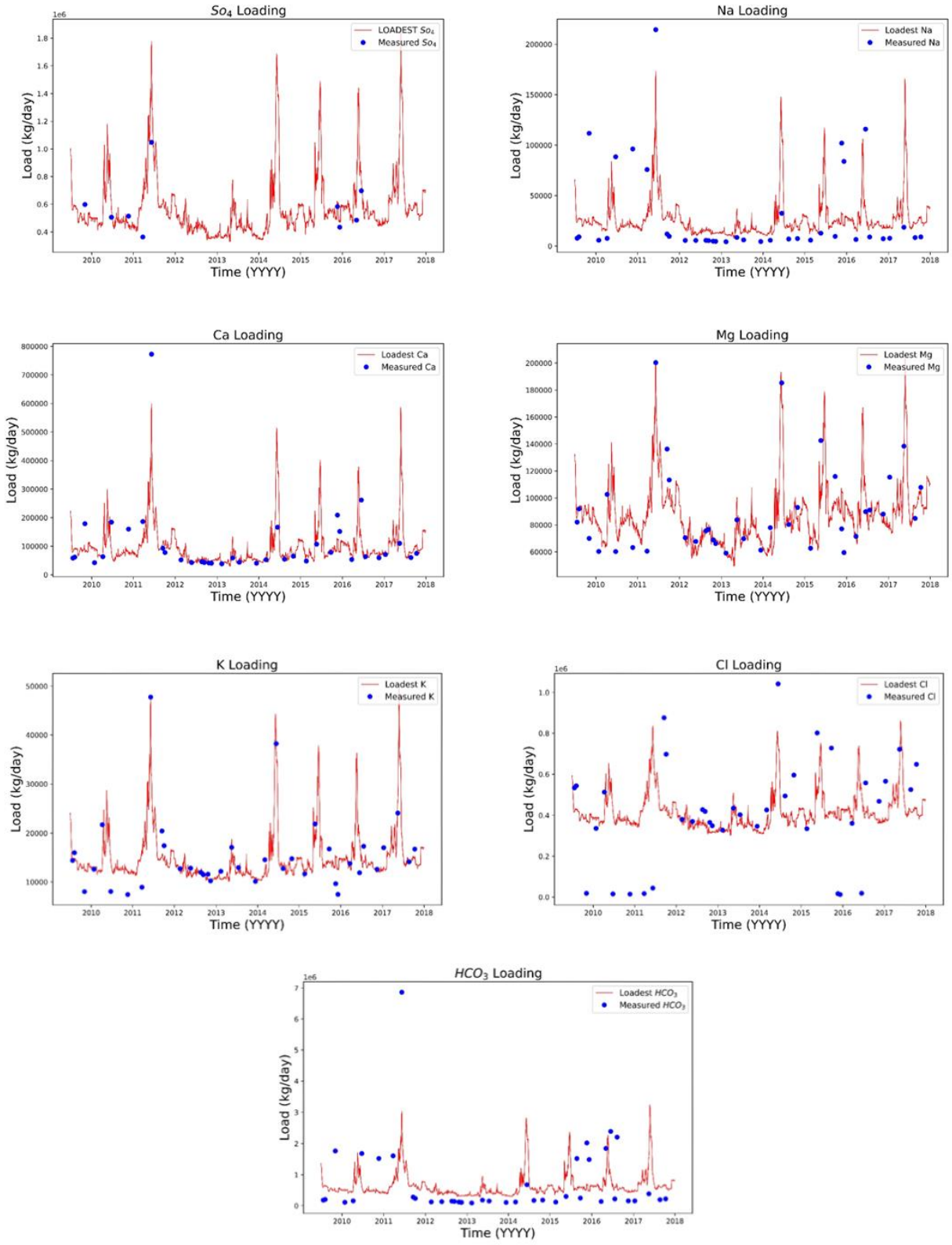

Figure 8: Represents the graphs comparing daily salt load estimates against the measured salt ion load for the corresponding day.

Due to lack of measured salt ion concentration in interior of watershed, the APEX-MODFLOW-Salt model is calibrated using only measured data at the outlet of the watershed. The model simulation period was between 2007 and 2017, and of this period from 2007 to 2009 model simulation was considered as warm up period to limit the influence of initial conditions such as soil water, soil salt content, streamflow, groundwater levels, and groundwater salt ion concentrations from influencing simulation during 2009-2017. The model was calibrated and validated for periods from 2009 to 2015 and 2015 to 2017, respectively. The APEX-MODFLOW-Salt model parameters were mainly calibrated based on monthly LOADEST estimates of SO_4 and Ca for variety of reasons. One such that was evaluation of performance metrics of LOADEST estimates of monthly salt loads from Table 3, says only Mg^{2+}, Ca^{2-} and SO_4^{2-} has R^2>60%, BP< ± 3.3 and NSE>0.45 altogether. The other reason was from study by (Bailey et al., 2022) said that in UCRB, price river watershed used in APEX-MODFLOW-Salt model simulated from 1995 to 2015 resulted that average annual total salt yield at outlet was 63,500 (Mg) of which 34,943 (55%) (Mg) and 9,360 (Mg) (14.7%) were SO_4^{2-} and Ca^{2-} respectively, together results approximately 70% of total salt yield in streams.

The initial GRW APEX-MODFLOW-Salt model's instream salt load daily simulation was averaged to monthly load to compare against the monthly salt load estimates computed by LOADEST to test the performance of the model. However, after performing visual analysis comparing the loads demanded manual calibration of few parameters. The soil and aquifer salt minerals parameter required to be calibrated were $CaSO_4$, $CaCO_3$, $MgSO_4$ & NaCl and seven salt ions concentration (SO_4^{2-}, Cl^-, HCO_3^-, Ca^{2+}, Na^+, Mg^{2+}, and K^+) present in soil water parameters were also included. The results of model parameters after calibration were heavily dependent on

visual comparison of temporal salinity loads from basin and statistical metrics like NSE, R^2 measuring model performance.

2.3 Quantifying Salinity Loads under Future Climate

The calibrated APEX-MODFLOW-Salt model of the GRW is supplied with future projected climate data to quantity changes in hydrology and salinity loads to the streams throughout the 21st century. In 2008, the Coupled Model Intercomparison Project Phase 5 (CMIP5) endorsed a set of 20 Global Climate Models (GCM) around the world with the aim to provide projections on changes in meteorology conditions at spatial and temporal scales are to recognize the impact of climate change on the ecosystem. The GCM is a type of numerical model that solves a set of complex mathematical equations to simulate the interaction between earth's energy balance components such as atmosphere, land surface, ocean, and sea ice. The large uncertain coarse horizontal resolution projection of GCM's meteorological data should be translated into relevant scale of local meteorological data for use in decision making and modeling studies. This process of converting the low-resolution output into a suitable near finer scale resolution for application is called downscaling, and one such type of statistical downscaling offering high computational efficiency is called Multivariate Adaptive Constructive Analog (MACA) method detailed in (Abatzoglou & Brown, 2012; Zhang et al., 2022)**.** Given its's ability to match by directly incorporating GCM's daily synoptic-scale field analog pattern with a catalog of observed synoptic-scale fields from observations rather than spatial interpolation to downscaled resolution follows the first principles of meteorology.

In this study (Abatzoglou & Brown, 2012; Zhang et al., 2022), the MACA downscaled meteorological variables were daily maximum and minimum temperatures, wind velocity, precipitation, and solar radiation. The historical observations from GRIDMET, 1950-2005

(Abatzoglou, 2013) were used for downscaling against the GCM's projection data. Initially, the quantile mapping based bias correction technique was applied to adjust the mean and variance of the GCM's daily data to GRIDMET using the projected and historical runs, then an epoch adjustment is made to remove the possibility of finding no analog in the historical period. Then, based on 30 years prediction patterns with a 45-day window around each calendar date, the best analog was found. While wind velocity and precipitation are scaled down independently, temperature and dew point are scaled together to improve coherence between the downscaled fields. To confirm that statistical moments are in conformity with observations, epoch modifications were once more applied, and quantile mapping was once more carried out. The final downscaled daily variable was the daily values achieved after quantile mapping detailed methods are available at (Abatzoglou & Brown, 2012; Zhang et al., 2022).

For our study, to include projected future MACA GCM datasets the spatial resolution of ~4km grid from 2018 to 2099 are obtained as CSV file for grid data from this public repository developed and maintained by the University of California MERCED (s://climate.northwestknowledge.net/MACA/data_csv.php). Since uncertainty in greenhouse gas concentration trajectory for future climate modelling prevails, therefore the GCM's are provided with two Representative Concentration Pathways (RCP) namely RCP 4.5 and RCP 8.5, where RCP 4.5 represents as a moderate carbon emission scenario in which greenhouse gas emissions peak around 2040 and later decline whereas RCP 8.5 represents "business as usual", highest baseline emissions scenes which continue to rise all the way through twenty-first century. Therefore, the APEX-MODFLOW-Salt model is supplied with both RCPs scenario GCM's climate projections to evaluate the future climate change impact on salt loading to the basin.

The variety of factors contribute to rise of large uncertainties in GCM climate projections, in that one such source is inter-model variability which has been assessed by comparing different GCM's at regional scales to observations (Giorgi & Francisco, 2000; Giorgi & Mearns, 2002; Hulme & Brown, 1998; Kittel et al., 1997; Stainforth et al., 2007; I. Smith & Chandler, 2010). Since there are 20 different GCM from CMIP5 climate projections MACA datasets available can be compared with the observations of the study region local scale to select a sub-set of available GCM's which better simulates the complex spatial patterns and seasonal and diurnal cycles of observed regional changes over a multidecadal timescales. The available 20 GCM MACA datasets are statistically compared with the historical rainfall data based on muti-criteria score based method for assessing the performance of GCM described detailed in (Fu et al., 2013)**.** The statistical measures used to evaluate the overall performance of GCM's are mean relative error (*MRE*), standard deviation relative error (*SDR*), normalized root mean square error (*NRMSE*), correlation coefficient (*Corr*), Brier score (*BS*), skill score (*S score*), and Kendall slope (*Kendall Slope)* and these statistical measures formulas are tabulated in table 4.

Table 4- The statistical criterion formula along with corresponding weighting factor assigned for evaluating GCM's is shown.

Statistical Criterion's	**Formula**	**Weighting Factor**
Mean Relative Error *(MRE)*	$\frac{m_{model} - m_{ob.}}{m_{ob.}}$	1.0
Standard Deviation Relative Error *(SDR)*	$\frac{\lvert Std_{model} - Std_{ob.}\rvert}{Std_{ob.}}$	1.0
Normalized Root Mean Square Error *(NRMSE)*	$\frac{\sqrt{\frac{1}{n}\sum_{i=1}^{n}(X_{mi} - X_{oi})^2}}{\sqrt{\frac{1}{n}\sum_{i=1}^{n}(X_{oi} - \bar{X}_{o})^2}}$	1.0
Correlation Coefficient *(Corr)*	Calculated Pearson Correlation in Python	1.0
Brier Score *(BS)*	$\frac{1}{n}\sum_{i=1}^{n}(P_{mi} - P_{oi})^2$	0.5
Skill Score *(S score)*	$\sum_{i=1}^{n} Minimum(P_{mi}, P_{oi})$	0.5
Kendall Slope	Calculated in Pro-UCL	1.0

These selected statistical criteria evaluate the accuracy of monthly climate variable in both magnitude and variance. Each GCM is ranked according to its resulting ranking score for each criterion. The total resulting ranking score for each GCM is calculated by summing all statistical criterion ranking score assuming same weights except for Brier score and Skill score are given weights 0.5 which evaluates the probability density function of climate variables shown in equation 3. The ranks are assigned in higher order to the lower total ranking score GCM's.

$$RS_{total} = RS_{MRE} + RS_{SDR} + RC_{NRMSE} + RC_{Corr} + RC_{Corr} + (0.5 \times RC_{BS}) + (0.5 \times RC_{S\ score}) + RC_{Kendal\ Slope} \quad \textit{(Equation 3)}$$

In our study region, spatially random three NOAA climate stations with varying altitudes shown in Figure 4**,** with adequate data have been selected to statistically evaluate its observed precipitation with MACA GCM's simulated precipitation**.** The three selected climate stations names are Crested Butte, CO US, Blue Mesa Lake, CO US and Delta, CO US respectively. All three climate stations are statistically analyzed using methods described in (Fu et al., 2013), and resulted same for top three GCM's ranking. The overall ranking and results for each considered GCM's for the climate station Crested Butte, CO US is shown in Appendix C Table 9**.** As with GCM's ranking results, the top three GCM models are MIROC-ESM_CHEM, IPSL-CM5B-LR and CanESM2 respectively. These three GCM's climate projection variables datasets for two greenhouse gas emissions scenario's RCP 4.5 and RCP 8.5 are obtained for specific locations grid in format of csv file. The Projected climate variables maximum temperature, minimum temperature, and precipitation from three GCM's are copied into the weather files of APEX (.DLY file), since it's a base modeling code for this integrated APEX-MODFLOW-Salt model.

The temporal trends of all three GCM's for both RCP projected climate variables as average annual maximum and minimum temperature (°C) and total annual precipitation (mm) are shown is Figure 9 along with historical climate records.

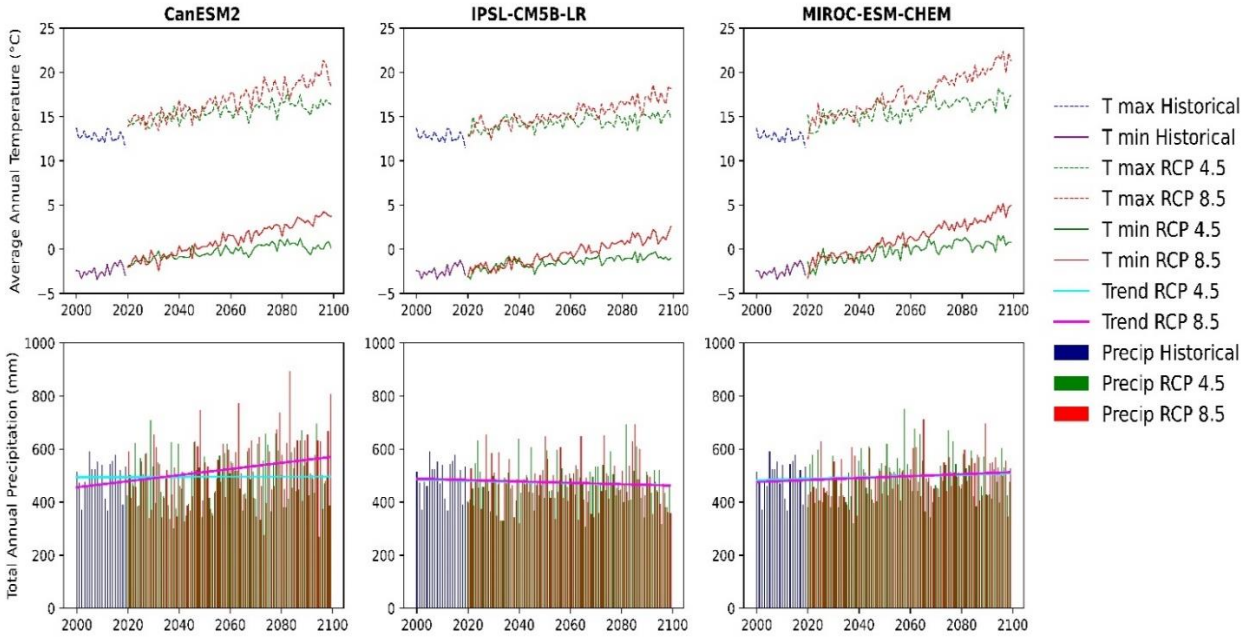

Figure 9- Average Annual Maximum and Minimum temperature (°C) and Total Annual Precipitation (mm) along with trendline for the statistically selected three Global Climate models CanESm2, IPSL-CM5B-LR and MIROC-ESM-CHEM for both RCP 4.5 and RCP 8.5 are shown in graph from 2020-2099 along with historical climate variables used in model input from 2000-2020 (Maximum temperature in dashed lines; RCP 4.5 and RCP 8.5 are consistently shown in green and red colors respectively)

From Figure 11, each climate model in both emission scenario clearly projects an increasing trend in annual average temperature throughout the 21st century, which agrees with previous studies (Lukas et al., 2014) reported the projection of 1.5-3°C warming by 2050 across Colorado. However, temperature trends for RCP 8.5 are greater regardless of all models. The yearly temporal pattern of precipitation simulations from GCM's for two scenarios are also not unanimous as temperatures throughout the 21st century. Total annual precipitation from CanESM2 RCP 8.5 shows the highest increasing trends in rainfall throughout the 21st century and MIROC-ESM-CHEM model shows very slight increasing trends for both RCP except all other models and scenario's shows same decreasing trends. This integrated APEX-MODFLOW-

Salt model with supplied GCM's climate attributes data is run from 2020 through 2099 for each of 6 scenarios (3 models each 2 RCP's), and the results of each simulation for hydrology and salinity loadings are assessed by comparison with the baseline scenario.

3. RESULTS AND DISCUSSION

3.1 Results of Hydrologic Modeling (APEX-MODFLOW)

The calibrated APEX-MODFLOW model simulated streamflow is plotted against the measured streamflow in a monthly time step manner for the GRW for several subarea gages in Figure 10. The calibration period is 2012-2017. These subarea stream gage sites and boundary delineations are shown in Figure 4. The APEX-MODFLOW model performance in our study is rated based on the general performance ratings by previous studies (Moriasi et al., 2007, 2015; Santhi et al., 2001), with monthly time step streamflow simulations considered as 'satisfactory' for NSE values ranging from 0.50 to 0.65, 'good' for ranges from 0.65 to 0.75 and anything greater than 0.75 is rated as 'very good'. However, in our watershed all of subarea's streamflow simulations NSE results seems satisfactory expect for subarea's 21 and 84, NSE values are 0.48 (under satisfactory range) and 0.69 (good) respectively. Consistently, all of subarea simulations are peaked during summer and low during winters since the hydrology of watershed is snowmelt and spring runoff. Despite the temporal patterns are matched consistently across the watershed, magnitude of flow peaks is mostly slight underestimated by the model, except for the outlet gage. Underestimation of peak flow could be due to the inadequate representation of daily weather data (e.g., precipitation), especially in mountainous, snowy regions. The streamflow comparison graph of subarea 64 which is the entire watershed outlet shows the simulated flow from model almost matches the pattern both temporal and peaks.

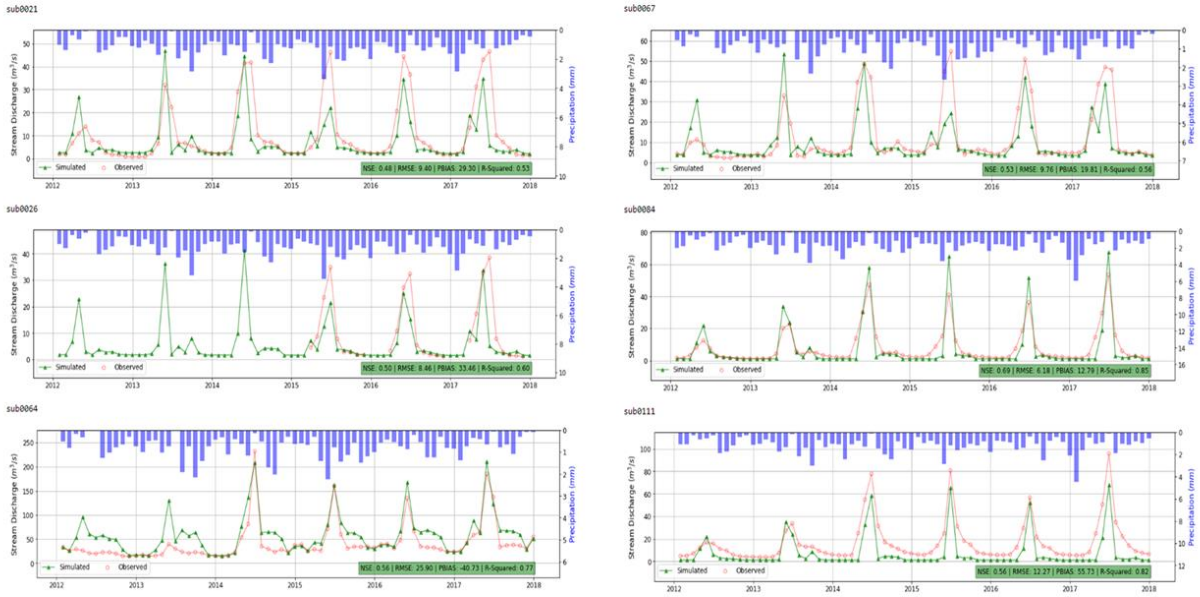

Figure 10: Monthly time series comparison graphs of simulated and observed streamflow (m3/s) for the Gunnison River Watershed based on APEX subareas. The Precipitation (mm) used in the model for respective subareas are also shown.

The MODFLOW output results for the GRW groundwater state variables such as groundwater head and saturated thickness (groundwater head – bedrock elevation) are mapped and shown in Figure11. Spatially varying groundwater head levels shown in Figure 11A almost mimics that topography of the study area in Figure 4. Corresponding areas with highest saturated thickness from Figure 11B subareas in Figure 5 receive the highest daily average precipitation could be reason for the high-water table recharge despite the low hydraulic conductivity since those area's geology is mostly sandstone and mudstone from Figure 1D. Figure 11C shows the annual average volume of groundwater discharges to surface water from aquifer by subareas through the simulation period 2007 to 2017. Despite the subareas with highest quantity of groundwater volumes delivered doesn't have high water table but those respective areas slope shown in Figure 1C are high in gradients.

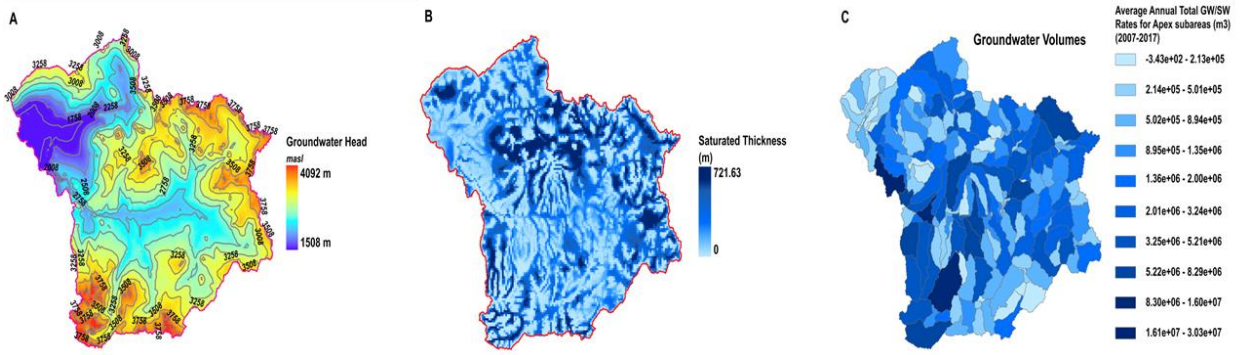

Figure 11- Groundwater modeling results for the GRW, (A) map showing cell by cell groundwater head elevation (m); (B) portrays cell by cell saturated thickness (m); and (C) depicts the average annual total groundwater volume rates delivered to APEX subarea streams by subareas for historical period 2007-2017

Figure 12 shows the time series of major hydrological components daily fluxes (m^3) attributes to streamflow volumes: surface runoff, quick return flow, surface water seepage to groundwater, groundwater discharge to surface water. Pie chart in same Figure 12 shows the apportionment of hydrology flux pathways to streamflow volumes. These results shows that major contributing factor to streamflow volumes in the GRW is surface runoff accounts for 65%, followed by quick return flow (a.k.a, lateral flow) 27% and net groundwater discharge to streams 8% respectively. These results prove the fact that watershed landscape has high gradients in slopes and most of the geologic deposits are granites (low hydraulic conductivity) except for downstream riverbeds are alluvium.

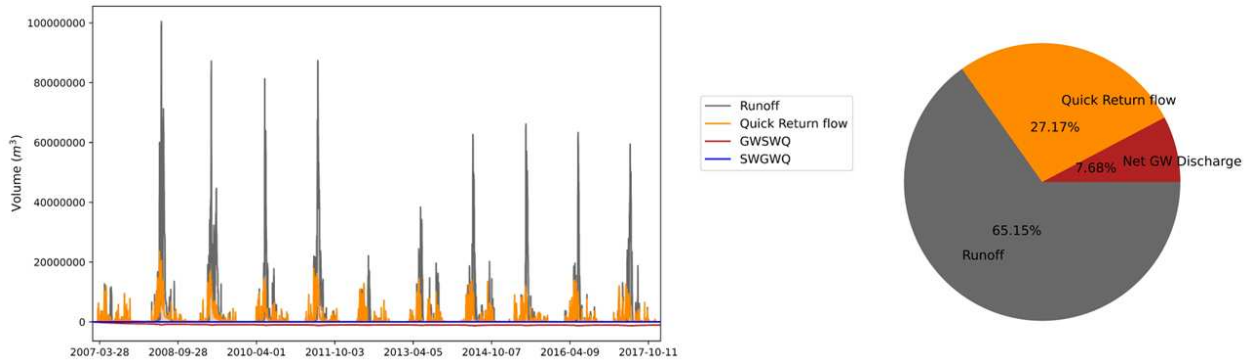

Figure 12- Time series graph depicts the daily volumetric hydrologic fluxes of surface runoff, quick return flow (combination of lateral flow and quick return flow) surface water seepage (SWGWQ) and groundwater discharge to streams (GWSWQ) for the

GRW during historical period simulation between 2007-2017; Pie-chart portrays the relative contributions of hydrologic fluxes on total watershed yield for the GRW.

3.2 Results of Salt Ion Transport Modeling (APEX-MODFLOW-Salt)

Simulated salt ions concentration from model results for the run period 2007 – 2017 is presented in Figure 13 along with the average of entire historical period of measured ion concentration in groundwater observation wells. However, available daily groundwater concentration measurements record ranges sporadically any day from year 1974 to year 2017 for all the spatially mapped wells in Figure 13. This limitation of data availability does not draw good comparison in magnitude for simulated ion concentration with measured concentration. However, the raster maps of simulated salt concentrations presented in order of TDS, SO_4, HCO_3, Cl and Ca from Figure 13 matches spatial distribution hotspots of measured wells indicating areas with high concentrations at northwest (near outlet), northern (for HCO_3, Cl) and portion in middle (for SO_4, Ca) of the watershed area. These areas of high salt concentrations simulated output matches with initial soil salt mineral fractions of $CaCO_3$ and $CaSO_4$ by subareas for APEX inputs in Figure 5 and these salt ions high concentration hotspots matching geology with shale, sandstone near outlet or north west part low lying area of watershed from Figure 1D, simulation agrees with the studies conducted by (Anning et al., 2007; Freethey & Cordy, 1991; Liebermann et al., 1989; Warner et al., 1985) compelling that high amount of dissolved solids to UCRB streams is sourced from Marine shales including Mancos shale than any other rocks.

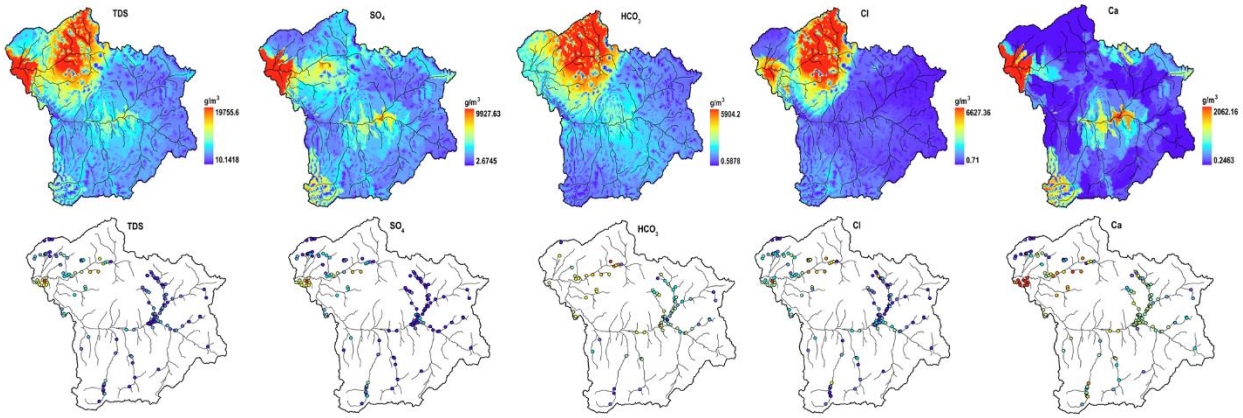

Figure 13- Top Row featuring Maps of cell by cell simulated groundwater concentration (g/m3) of Total dissolved solids (TDS), Sulphate (SO4), Bicarbonate (HCO3), Chloride (Cl) and Calcium (Ca) for the year 2017; Bottom row featuring measured groundwater concentration (g/m3) for same all above ions in the same order from the network of USGS groundwater observation wells.

The monthly time series comparison of in river salt load simulated at outlet gage is plotted against the LOADEST estimation loads, e.g., measured loads of salt ions with uncertainty in Figure 14. Through model calibration, the graph in Figure 14 shows that simulated salt loadings match the temporal pattern of the observed loadings and mostly unmatching the high magnitude peaks. The model performance metrics, Coefficient of determination (R^2) and Correlation coefficient values (r^2) for each ion are presented in same Figure 16, including both calibration and validation period values ranges from 0.04 to 0.30 and 0.19 to 0.54 for Mg and HCO_3 respectively. Low performance indicates the model's inability to simulate the high peak magnitude of salt loadings due to underestimation of streamflow since model limits the applicability of hourly intense precipitation inputs.

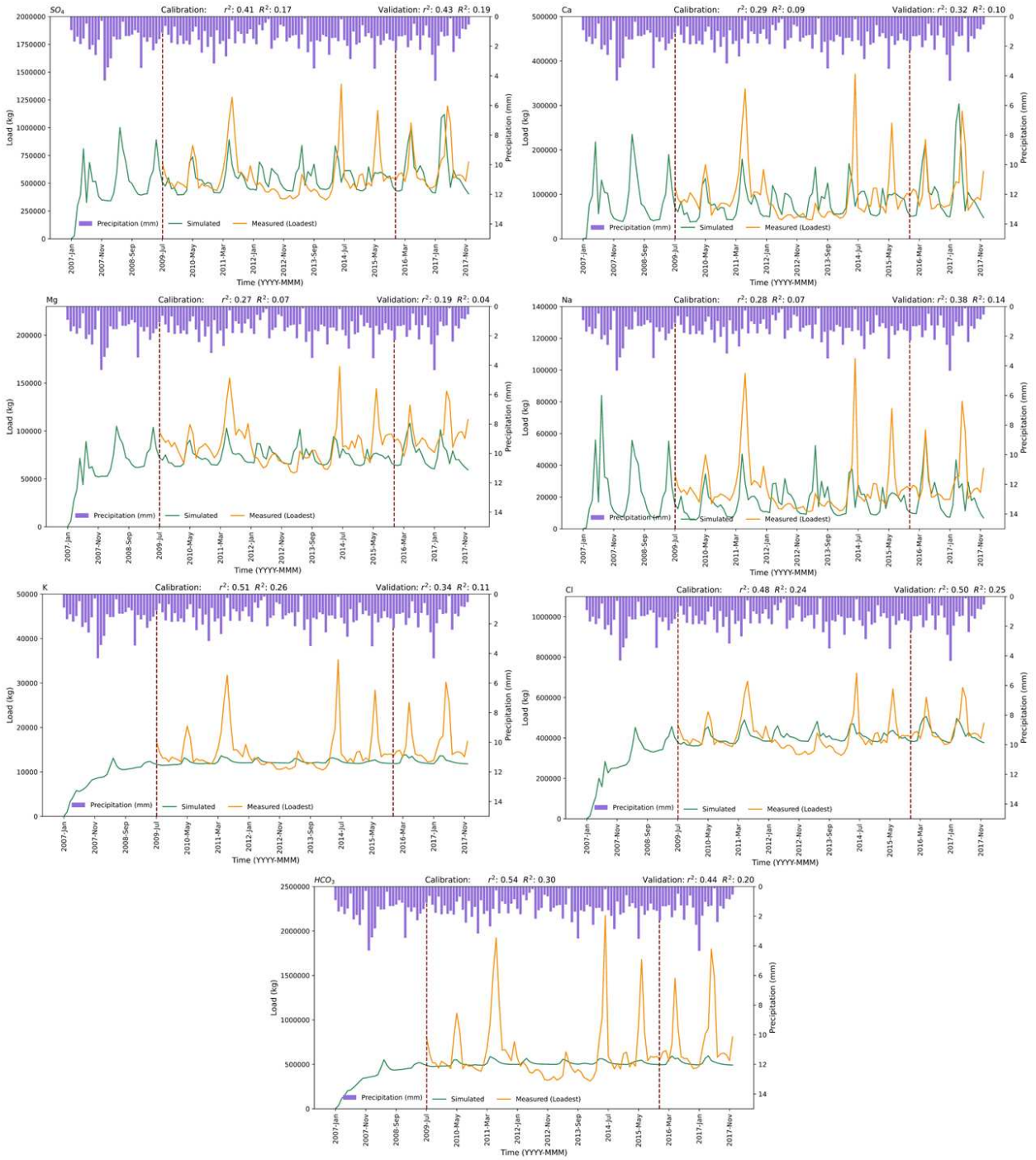

Figure 14- Time series graphs of simulated and measured mean monthly in-river loads (kg) at the watershed outlet (subarea 64 – USGS gage location) for the 6 ions (SO4, Ca, Mg, Na, K, Cl, HCO3) for which historical measured concentration (g/m3) values are available along with basin wide monthly mean precipitation(mm) on secondary axis. The chart is provided with model performance metrics: correlation coefficient (r2) and coefficient of determination (R2) for calibration period (July 2009 – December 2015) and validation period (January 2016 – December 2017). The model simulated for in-stream salinity loadings from January 2007 – July 2009 is considered as Warmup period.

As a result of precipitation, these salt minerals from soil profile dissolute to soil water which increases salt storage in soil mass which then transported via different hydrological fluxes: Surface runoff, Rainfall erosion, Lateral flow, Quick return flow and leaches salt mass to the aquifer water table delivered through groundwater discharge to the streams. For the GRW, from Figure 15, almost 73% of total salt load delivered to streams is through Groundwater discharge, followed by quick return flow 16%, lateral flux 9% and negligible percent from erosional runoff and Surface runoff. Since high rainfall events drive the fluxes in erosional runoff, surface runoff, lateral flow and quick return flow, whereas this consistent loadings of fluxes through groundwater discharge are due to high maintained groundwater gradients to the stream. these results seem to accord with reports from other studies (Bailey et al., 2021; Rumsey et al., 2017), in both statistical modeling of entire UCRB and same APEX-MODFLOW-Salt modeling of the Price River watershed (HUC 8 in UCRB) results 89% of salt loads comes from groundwater discharge to rivers. These salinity baseflow fraction results agree with (Nauman et al., 2019; Rumsey et al., 2017), said significant contributions of salinity in UCRB is from groundwater.

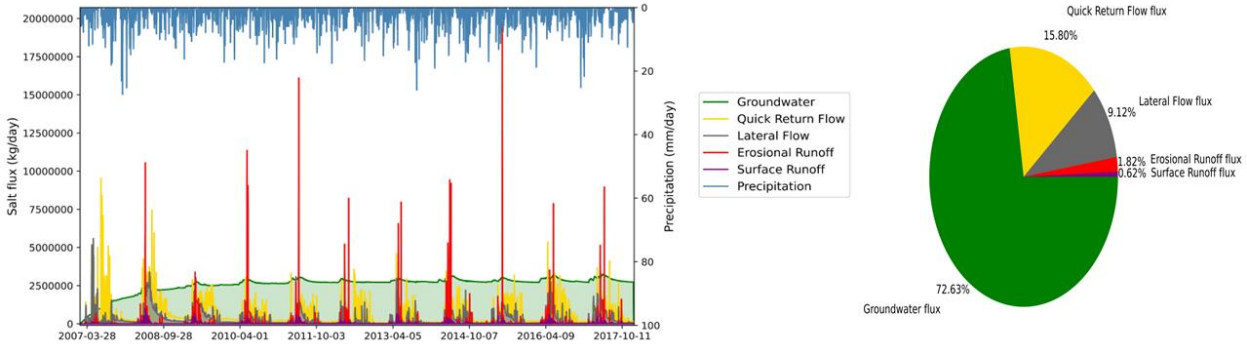

Figure 15- Time series graph features the mass of daily salt loading results (kg/day) for the entire GRW by surface runoff, rainfall erosional runoff, soil lateral flow, quick return flow and groundwater discharge with respect to the source daily precipitation (mm/day) on secondary axis from 2007 to 2017; Pie-chart shows the salt mass source apportionment.

The maps in Figure 16 shows the subareas of high salt loadings to the river network through hydrologic pathways quick return flow and groundwater discharge for the ions SO_4,

HCO_3, Cl and Ca. These loadings from subareas match with areas of simulated high concentrations for each corresponding salt ions. Figure 17 shows the maps of total salinity loads transported through each hydrologic pathway for the GRW. Spatially distribution of loads transported from each subarea are highlighted for each hydrologic pathway for the simulation period. These comprehensive maps indicate that areas of high loading occur mostly through northwest, north and middle regions of the watershed.

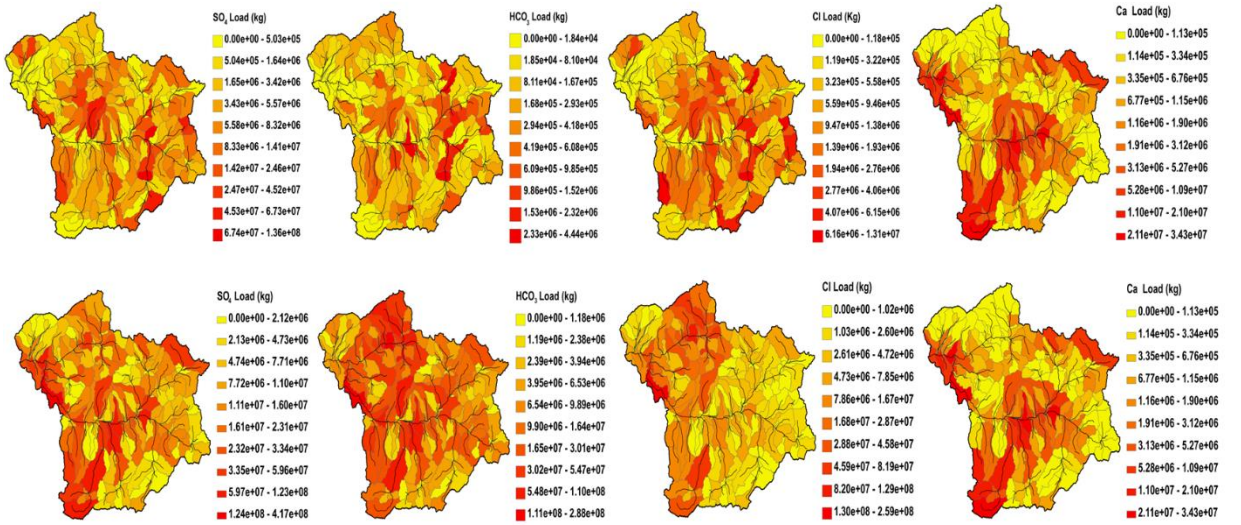

Figure 16- Top Row Maps featuring the sum of daily salt mass loading results for quick return flow by subarea in order of Sulphate (SO4), Bicarbonate (HCO3), Chloride (Cl) and Calcium (Ca) for the simulation period of 2007 – 2017. Bottom Row Maps featuring the sum of daily salt mass loading results for groundwater discharge by subarea in order of Sulphate (SO4), Bicarbonate (HCO3), Chloride (Cl) and Calcium (Ca) for the simulation period of 2007 – 2017.

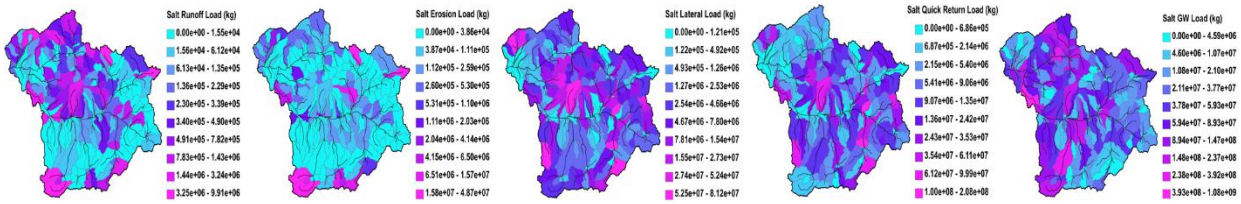

Figure 17- Maps shows the total daily salt mass loading results for the simulation period of 2007-2017 for surface runoff, rainfall erosion, lateral flow, quick return flow, net groundwater discharge to streams by subarea.

Table 5 presents the results of percent contribution of each hydrologic flux pathways for each salt ions. For HCO_3 and K, High percent of loads delivered to river through groundwater

discharge whereas for Na relatively low percent of loads delivered. This result is because APEX salinity equilibrium chemistry module's precipitation dissolution feature of salt minerals doesn't include stoichiometric algorithm approach for HCO_3 and K. High solubility product parameters for NaCl is 37.3, which affects the dissolution of soil salt mineral causing Na to get dissolved quickly during rainfall events and transports primarily through lateral flow and quick return flow before leaches to the water table in aquifer.

Table 5- The Percent contribution of the salt mass hydrologic pathways source to streams for the eight simulated salt ions for the Gunnison River Watershed; Ions are arranged in order of load discharge magnitude for the Gunnison River watershed where highest contributing at first.

Salt Ions	**Surface Runoff (%)**	**Erosional Runoff (%)**	**Lateral Flow (%)**	**Quick Return Flow (%)**	**Groundwater (%)**
SO_4	1	2	14	24	60
HCO_3	0	0	1	1	98
Cl	0	2	5	9	84
Ca	2	1	20	34	44
Mg	1	3	8	14	74
CO_3	15	3	9	12	61
Na	2	14	24	41	20
K	0	0	1	2	97

From our model simulation 2007 - 2017, yearly average sum of all modeled salt ions exported from the outlet of the watershed is 582 million kg/year. Of that where SO_4, HCO_3, Cl and Ca alone accounted for 39.4 %, 25.6 %, 17.5% and 8.4% respectively, and remaining other ions relative contribution to the total load is presented in Figure 18 along with the daily time series of each salt ions yield (kg/day). Since the average annual salt yield estimated from the UCRB reported by Nauman et al. 2019 is 5,430 M Kg, based on our model simulation results for the GRW relatively contributes salt of about 10.72% to the entire UCRB with area being relatively 5% to the UCRB.

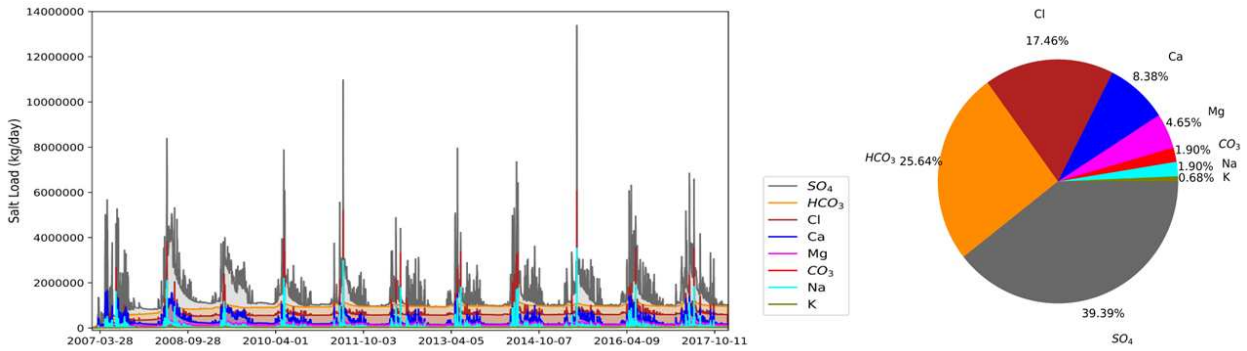

Figure 18- Time series graph features the daily simulated salt yield (kg/day) by salt ion from the Gunnison River Watershed; Pie-chart portrays the respective salt ion apportionment, from 2007 to 2017.

3.3 Changes in Hydrology and Salt Loading under Future Climate Scenarios

The calibrated APEX-MODLFOW-Salt integrated model supplied with each GCM's projected climate variables from 2020 to 2099 simulation run results and their key findings of relative changes in hydrology and salinity loading from modeled baseline scenario 2007-2017 are reported in Table 5. Each model run with different scenario's input yields different average annual water yield (mm/year) and average annual salt exported from the basin outlet (M kg/year). CanESM2 RCP 8.5 and IPSL-CM5B-LR RCP 8.5 model scenario run simulates highest and lowest average annual water yield (mm/year) among other model runs 117.91 (mm/year) and 95.14 (mm/year) respectively which is relatively +7.32% and -13.40% from historical baseline scenario. From relative changes in the water yield and the salinity export to the stream from baseline scenario says that the hydrology and salt load transport simulation is directly proportional to the forcing weather variables since Figure 9 clearly shows the increasing precipitation trends for CanESM2 RCP 8.5 and decreasing trends for IPSL-CM5B_LR both RCPs respectively. Despite few scenarios depicts increasing water yield from baseline scenario and other scenarios decreasing but apportionment of hydrologic flux path to the streamflow generation in the model for the surface flow decreasing and subsurface flow which is the

combination of both horizontal return flow (quick return flow) and aquifer return flow (groundwater discharge) increasing unanimously across all the model runs. Since increase in surface temperature across the 21st century affects evapotranspiration rate (Hargreaves method is used here) which impact soil field capacity forces higher infiltration rate increases contribution to baseflow than surface flow.

Table 6- Relative Changes in Hydrology and salinity loadings to the GRW for each of three GCM inputs for both RCP from baseline scenario and Percent of hydrology and salinity exported to stream due to each pathway.

Salt Mass								**Hydrology**				
% Of watershed salt mass exports due to flux pathways								**% Of Hydrologic flux transport from the GRW**		**Average Annual Salt exported from Basin Outlet. (M kg/year)**	**% Change from Baseline**
Surface Runoff	**Erosional Runoff**	**Lateral Flow**	**Quick Return Flow**	**Groundwater Discharge**				**Quick Return Flow**	**Groundwater discharge**		
0.62	1.82	9.13	15.81	72.62				27.18	7.68	582.43	
3.02	1.63	7.68	16.33	71.34				28.79	8.29	615.31	5.64
2.95	1.47	7.13	13.85	74.60				28.17	7.94	638.21	9.58
2.98	1.88	7.41	16.00	71.74				29.31	9.20	606.14	4.07
2.80	1.71	8.06	18.03	69.39				29.92	9.42	614.79	5.56
2.83	1.86	7.93	16.62	70.76				29.86	9.41	612.42	5.15
2.57	1.62	8.13	17.03	70.65				30.57	8.94	618.18	6.14

Climate Inputs Scenario	RCP	Average Annual Water Yield (mm/year)	% Change from Baseline	Surface Runoff
Baseline		109.86		65.14
CanESM2	4.5	111.97	1.92	62.91
	8.5	117.91	7.32	63.88
IPSL-CM5B-LR	4.5	98.74	-10.13	61.48
	8.5	95.14	-13.4	60.66
MIROC-ESM-CHEM	4.5	105.46	-4.02	60.73
	8.5	99.67	-9.28	60.48

In contrast to water yield relative changes from baseline across the models, the average annual salt exported from the basin outlet increases consistently for all the scenario models. The average annual highest and lowest contributing salt load (M kg/year) from basin outlet is 638.21 M kg/year from CanESM2 RCP 8.5 and 606.14 M kg/year from IPSL-CM5B-LR RCP 4.5 respectively. Despite the model IPSL-CM5B-LR RCP 8.5 give in lowest annual average water yield (mm/year) compared with other scenarios, this model exports salt from basin is 614.79 M kg/year not the lowest contributing model. This is because the groundwater discharge contribution to streamflow generation is 9.42% which is +2.4% than groundwater discharge from IPSL-CM5B-LR RCP 4.5 likewise +2.08% for quick return flow. Since from Figure 17 the baseline historical model the highest salt exported flux pathway for the GRW is groundwater flux (73.62%) followed by quick return flow (15.81%).

Inspecting 5 flux pathways (groundwater flow, quick return flow, soil lateral flow, rainfall erosional runoff. and surface runoff) contributing to in-stream salt mass for all different

future scenario's consistently transport same apportionment with negligible differences except for CanESM2 RCP 8.5, this model relatively low contribution from quick return flow flux is offset by groundwater discharge flux (both are part of subsurface flow). However, these scenario models simulation across 21st century changes salt apportionment of surface runoff flux and soil lateral flow flux from baseline model which are increasing and decreasing.

The 21st century time series of watershed wide total annual salt load simulation and their relative contribution of total landscape mass exports due to each pathway for the selected scenario models CanESM2 RCP 8.5 and IPSL-CM5B-LR RCP 4.5 are shown in Figure 19 for each year. The solid lines of salt flux pathways represent the contributions of landscape salt from each pathway for CanESM2 RCP 8.5 whereas dashed line represents the IPSL-CM5B-LR RCP 4.5. Groundwater flux discharge of salt mass still dominate this watershed, however the temporal pattern of groundwater flux loadings to the stream consistently decreases, whereas salt loaded though quick return flux discharge consistently increases from 2nd half of the 21st century. Soil lateral flow is the third dominant salt discharge which are consistent with time series except for few spikes after 2-5 years from the year witnessed high total annual rainfall event in Figure 9. Despite the soil lateral flow and quick return flow being the horizontal subsurface flow in hydrology cycle, the distinguished differences between them are that lateral subsurface flow makes its path to its downstream subarea soil water storage whereas quick return flow gets return to the channel flow in same subarea. The few spikes in quick return flux discharge around 2048 – 2052 and high consistent loading from 2084-2099 is due that the subsurface flow in hydrology has greater delayed time reaching stream after high total storm events in Figure 17 typical after 2- 5 years and consistent throughout the simulation. This emphasis that short period independent storm events (months or seasons) influences salt transport through horizontal subsurface flow

and the consistent years or decades periods of salinity discharge governed by groundwater flux is due to average annual rainfall- recharge events.

Comparing 21st century annual time series with baseline scenario daily series salt load discharge in Figure 17, proves that the increasing precipitation intensity over short period of simulation results in high magnitude peak loads from rainfall erosional runoff, but the salt from this pathway exports salt in lesser scale than from groundwater discharge, quick return flow and lateral flow for longer periods in overall salinity loadings (decade or century). This is evident with the watershed wide, average annual leaching of salt mass stored in soil profile for the scenario models CanESM2 RCP 8.5 and IPSL-CM5B-LR RCP 4.5 increases 128% and 107% from baseline scenario respectively, resulting in higher groundwater salt mass and subsequent higher groundwater salt loads to the streams. This overall scenario model's simulation results compare well with other UCRB statistical modeling studies. Rumsey et al. (2017) said that despite the baseflow accounting for less than 50% for streamflow, 89% of dissolved in-stream solid salt mass is loaded through groundwater discharge. Also, Nauman et al. (2019) said that the total estimate of 1.4% in-stream loading comes from exposed high bare rangeland via surface runoff and erosion runoff, but for our watershed future scenario's simulation results not more 4.9% from these two hydrology pathways. This increased salt mass discharge is due to the higher fraction of slope gradient, rangeland and impervious subsurface compared to average UCRB watershed.

CanESM2 RCP 8.5 simulation run for 21st century resulting hydrology and salinity loading regime relative changes from baseline historical scenario 2007-2017 for groundwater volumes discharge and salinity load to the stream through groundwater flux and quick return flux varying spatially in subareas for mean daily temporal scale are shown in Figure 20. From maps

in Figure 20 A. highlights the subareas that experience changes in hydrology pattern of mean daily groundwater discharge to streamflow at end of 80-year simulation from the baseline scenario. The relative change value -98.96% to -0.11% indicates that for baseline scenario 2007-2017 corresponding subareas had initially water infiltrate to recharge aquifer water table from surface water, however after this scenario's simulation water table for those subareas have risen enough to drive the water from aquifer table to the stream to maintain groundwater gradients with stream. Also, higher percent increase in groundwater delivered to the stream are subareas that are located immediately below high elevated surrounding subareas from Figure 1 & Figure 4 and the confluence of tributaries starting from those subareas forming mainstream at this subarea, especially higher percentage of increase in groundwater volumes in subareas are mostly in north and northeast part of the watershed which is a low-lying area for the entire basin. From Figure 20 B, the subareas that experience high percent of change in groundwater salt loadings to stream are the same subareas that experienced high increase in groundwater volumes. Figure 20 C depicts the subareas that experience over two orders of magnitude of relative percent increase in quick return salinity discharged to the stream from baseline scenario 2007 - 2017.

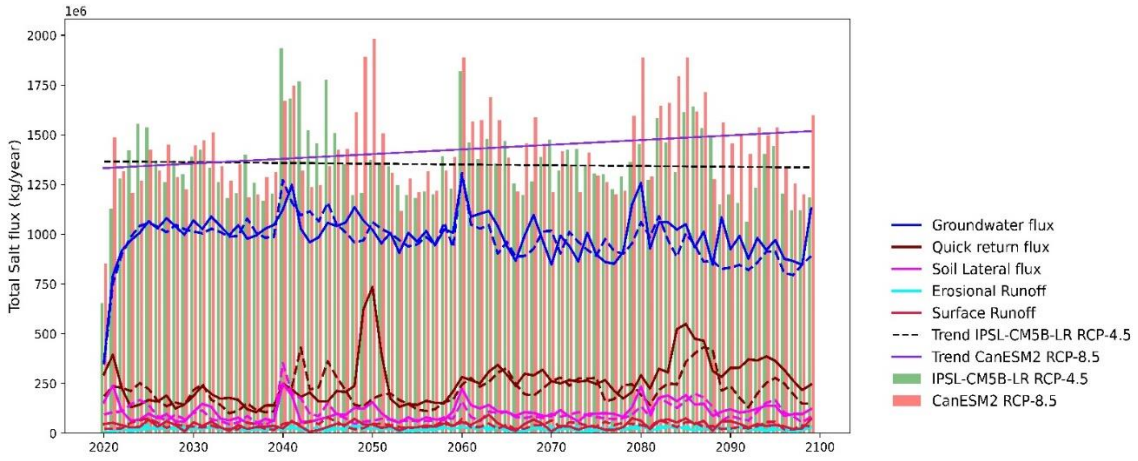

Figure 19- The watershed wide annual total salt mass exported by CanESM2 RCP 8.5 (red) and IPSL-CMB-LR RCP 4.5 (green) are shown as bar chart along with their trends and the temporal relative contributions of salt from each flux pathways for two GCM scenarios (illustrated by dashed line for IPSL-CM5B-LR RCP 4.5 and solid line for CanESM2 RCP 8.5) are shown.

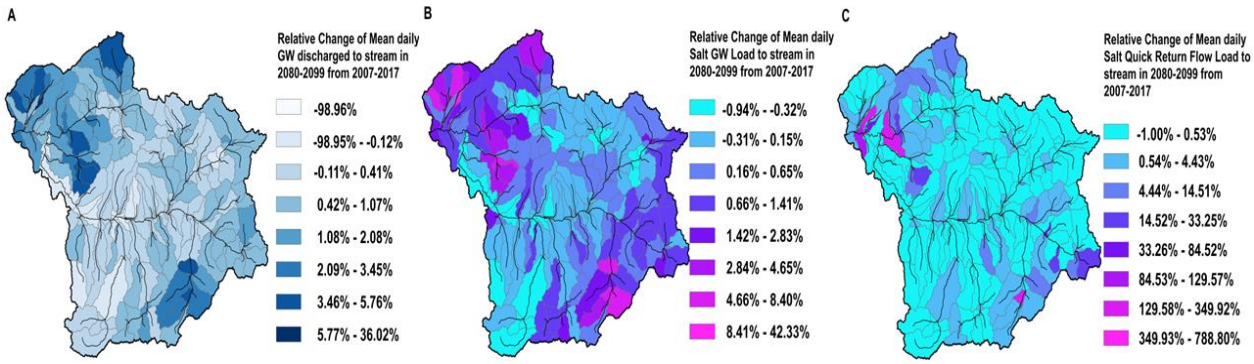

Figure 20- GRW Maps of Relative changes in (A) Mean Dailey Groundwater discharged to stream; (B) Mean Daily Groundwater salt flux delivered to stream; (C) Mean Daily Quick Return salt flux delivered to stream for the CanESM2 RCP 8.5 simulation results 2080-2099 against baseline scenario 2007-2017 simulation run.

3.4 Study Limitations

Although the APEX-MODFLOW-Salt model for the baseline scenario captures the spatial and temporal pattern of hydrology and salt ion fate and transport processes on comparison with measured physical data and results from relevant studies (Bailey et al., 2022, 2021), there are certain assumptions used in preparing the input data for the model simulation introduces lot of uncertainties with the results. List of limitations includes the following:

1) Initial soil salt minerals and Initial salt in groundwater salt ion concentration are inherently uncertain from predictive soil property maps by USGS and soil water ion concentration from relatively sparse network of observation cells without timely measurements from NWIS. These inputs are sourced from sources that are not physically measured or measured sporadically with possibly faulty device.

2) Without abundant physically measured streamflow discharge and salt ion concentration in groundwater observation wells from interior points at varying altitudes in the watershed, the strong testing of model is not possible. Salinity simulations are tested

against LOADEST estimation results for salt ions which is a statistically model requires the inputs of physically measured soil water salt concentrations.

3) Use of statistically downscaled MACA climate datasets for running future climate scenario's simulations stems from model, spatial, temporal and data processing uncertainties. Despite the uncertainties in climate projection accuracy among the models are lessened using statistical evaluation criteria, different climate model yields different climate output for same historical climate input.

4) The simulations throughout the 21st century assumes land cover and land use remains constant. The realistic setting of the GRW includes lots of irrigation practices at low lying elevation and reservoir influenced instream hydrology and salt ion fate and transport process are not simulated due to lack of data availability.

5) Since all available GCM's results in increase in temperature on an average of about 3 – 6 °C at the end of 21st century. However, this study didn't use the information of solar radiation, relative humidity and windspeed for the future scenario in simulating accurate evapotranspiration rate for the GRW.

4. SUMMARY AND CONCLUSIONS

In this study, the integrated hydro-chemical watershed model APEX-MODFLOW-Salt is used to assess the spatio-temporal patterns of hydrology and salt ion transport in the GRW (14,608 km^2) of the UCRB and quantify the effects of climate change on these patterns and magnitudes during the 21st century. The historical model simulation results for 2007-2017 were tested against monthly streamflow and in-stream salt loading at the watershed outlet, whereupon the model was forced by downscaled precipitation and temperature output from selected Global Climate Models for assessment of hydrologic fluxes and salt loadings through the end of the 21st century. Salt loadings to the river system occur via surface runoff, rainfall erosional runoff, soil lateral flow, and groundwater discharge. Key insights from results include:

- *Historical period*: Although streamflow is sourced predominantly by surface runoff (65% of total water yield, compared to 27% quick return flow and 8% from groundwater), salt loads in the Gunnison River are sourced mainly from the aquifer (73% from groundwater discharge, compared to 15% from quick return flow). The higher groundwater salt loads are due to higher salt ion concentrations in groundwater, as compared to surface runoff. These results, i.e., high salt loading contribution from groundwater, agree with the studies from Rumsey et al. (2017) for the entire UCRB and Bailey et al. (2021) for the Price River Watershed, also in the UCRB.
- *Historical period*: Average annual salt exported from watershed is 582.43 M kg, equal to 10.7% of total salt yielded from the UCRB, using values from Nauman et al. (2019). The GRW account for only 5% of the total UCRB area. Of the total salt yield, SO_4, HCO_3, Cl and Ca accounted for 39.5%, 25.6%, 17.5% and 8.4% (91%), respectively, of total salt,

due to the prevalence of gypsum and calcite in the soils and geologic units (shale, sandstone, and mudstone) of the watershed.

- *Future Climate*: Although the two GCMs CanESM2 RCP 8.5 and IPSL-CM5B-LR RCP 8.5 resulted in a respective increase (+7.3%) and decrease (-13.4%) in average annual water yield from the baseline scenario, both models produced an increased contribution from subsurface flow to streams and a decreased contribution from surface runoff. Due to an increase in soil salinity, and hence salt ion concentrations in surface runoff, salt ion loading to streams via surface runoff increased for both models.
- *Future Climate*: The CanESM2 RCP 8.5 model yields the highest increase in salt loads: +9.6% from the historical period. The average annual salt exported is 638.21 M kg/ is due mainly to increases in surface runoff loads groundwater loads (Table 6).
- *Future Climate*: In the end of the century, the CanESM2 RCP 8.5 scenario depicts that the subareas that undergo significant relative changes in groundwater discharge and salt ion loading to streams are located immediately below high-elevation subareas.

From these results we conclude that future climate can exacerbate salinity conditions in semi-arid regions due to increases in surface runoff salinity and groundwater discharge salinity. Effects vary by location, depending on topography, soil type, geologic units within the aquifer system, and precipitation patterns. The APEX-MODFLOW-Salt model can be used as a tool in the decision-making process for water and watershed managers, as solutions are sought for mitigating downstream salinity pollution. The modeling procedure can be applied to any semi-arid watershed and river basin to identify salt afflicted hotspots and apply general salinity mitigation under management practices.

REFERENCES

Abatzoglou, J. T. (2013). Development of gridded surface meteorological data for ecological applications and modelling. *International Journal of Climatology*, *33*(1), 121–131.

Abatzoglou, J. T., & Brown, T. J. (2012). A comparison of statistical downscaling methods suited for wildfire applications. *International Journal of Climatology*, *32*(5), 772–780.

Abbas, A., Khan, S., Hussain, N., Hanjra, M. A., & Akbar, S. (2013). Characterizing soil salinity in irrigated agriculture using a remote sensing approach. *Physics and Chemistry of the Earth*, *55–57*, 43–52. https://doi.org/10.1016/j.pce.2010.12.004

Anning, D. W., Bauch, N. J., Gerner, S. J., Flynn, M. E., Hamlin, S. N., Moore, S. J., Schaefer, D. H., Anderholm, S. K., & Spangler, L. E. (2007). *Dissolved solids in basin-fill aquifers and streams in the southwestern United States*. US Geological Survey.

Bailey, R. T., Jeong, J., Park, S., & Green, C. H. M. (2022). Simulating salinity transport in High-Desert landscapes using APEX-MODFLOW-Salt. *Journal of Hydrology*, *610*(April), 127873. https://doi.org/10.1016/j.jhydrol.2022.127873

Bailey, R. T., Tasdighi, A., Park, S., Tavakoli-Kivi, S., Abitew, T., Jeong, J., Green, C. H. M., & Worqlul, A. W. (2021). APEX-MODFLOW: A New integrated model to simulate hydrological processes in watershed systems. *Environmental Modelling and Software*, *143*(June), 105093. https://doi.org/10.1016/j.envsoft.2021.105093

Bailey, R. T., Tavakoli-Kivi, S., & Wei, X. (2019). A salinity module for SWAT to simulate salt ion fate and transport at the watershed scale. *Hydrology and Earth System Sciences*, *23*(7), 3155–3174. https://doi.org/10.5194/hess-23-3155-2019

Cadaret, E. M., Nouwakpo, S. K., McGwire, K. C., Weltz, M. A., & Blank, R. R. (2016). Experimental investigation of the effect of vegetation on soil, sediment erosion, and salt transport processes in the Upper Colorado River Basin Mancos Shale formation, Price, Utah, USA. *Catena*, *147*, 650–662. https://doi.org/10.1016/j.catena.2016.08.024

Cañedo-Argüelles, M., Kefford, B. J., Piscart, C., Prat, N., Schäfer, R. B., & Schulz, C. J. (2013). Salinisation of rivers: An urgent ecological issue. *Environmental Pollution*, *173*, 157–167. https://doi.org/10.1016/j.envpol.2012.10.011

Clement, T. P. (1999). *A modular computer code for simulating reactive multi-species transport in 3-dimensional groundwater systems*. Pacific Northwest National Lab.(PNNL), Richland, WA (United States).

Corwin, D. L. (2021). Climate change impacts on soil salinity in agricultural areas. *European Journal of Soil Science*, *72*(2), 842–862. https://doi.org/10.1111/ejss.13010

Doherty, J. (2018). Model-Independent Parameter Estimation User Manual Part I: PEST. *SENSAN and Global Optimisers*.

Dugan, H. A., Bartlett, S. L., Burke, S. M., Doubek, J. P., Krivak-Tetley, F. E., Skaff, N. K., Summers, J. C., Farrell, K. J., McCullough, I. M., Morales-Williams, A. M., Roberts, D. C., Ouyang, Z., Scordo, F., Hanson, P. C., & Weathers, K. C. (2017). Salting our freshwater

lakes. *Proceedings of the National Academy of Sciences of the United States of America*, *114*(17), 4453–4458. https://doi.org/10.1073/pnas.1620211114

Freethey, G. W., & Cordy, G. E. (1991). *Geohydrology of Mesozoic rocks in the Upper Colorado River Basin in Arizona, Colorado, New Mexico, Utah, and Wyoming, excluding the San Juan Basin*. US Government Printing Office.

Fu, G., Liu, Z., Charles, S. P., Xu, Z., & Yao, Z. (2013). A score-based method for assessing the performance of GCMs: A case study of southeastern Australia. *Journal of Geophysical Research: Atmospheres*, *118*(10), 4154–4167.

Ghassemi, F., Jakeman, A. J., & Nix, H. A. (1995). *Salinisation of land and water resources: human causes, extent, management and case studies.* CAB international.

Giorgi, F., & Francisco, R. (2000). Evaluating uncertainties in the prediction of regional climate change. *Geophysical Research Letters*, *27*(9), 1295–1298.

Giorgi, F., & Mearns, L. O. (2002). Calculation of average, uncertainty range, and reliability of regional climate changes from AOGCM simulations via the "reliability ensemble averaging"(REA) method. *Journal of Climate*, *15*(10), 1141–1158.

Hargreaves, G. H., & Samani, Z. A. (1985). Reference crop evapotranspiration from temperature. *Applied Engineering in Agriculture*, *1*(2), 96–99.

Hassani, A., Azapagic, A., & Shokri, N. (2020). Predicting long-term dynamics of soil salinity and sodicity on a global scale. *Proceedings of the National Academy of Sciences of the United States of America*, *117*(52), 33017–33027. https://doi.org/10.1073/PNAS.2013771117

Hock, R. (2003). Temperature index melt modelling in mountain areas. *Journal of Hydrology*, *282*(1–4), 104–115. https://doi.org/10.1016/S0022-1694(03)00257-9

Hoegh-Guldberg, O., Jacob, D., Taylor, M., Bindi, M., Brown, S., Camilloni, I., Diedhiou, A., DJalante, R., Ebi, K. L., Engelbrecht, F., Guiot, J., Hijioka, Y., Mehrotra, S., Payne, A., Seneviratne, S. I., Thomas, A., Warren, R., & Zhou, G. (2018). Impacts of 1.5{\textdegree}C Global Warming on Natural and Human Systems. *World Meteorological Organization*, 175–311.

Hosseini, P., & Bailey, R. T. (2022). Investigating the controlling factors on salinity in soil, groundwater, and river water in a semi-arid agricultural watershed using SWAT-Salt. *Science of the Total Environment*, *810*, 152293. https://doi.org/10.1016/j.scitotenv.2021.152293

Hulme, M., & Brown, O. (1998). Portraying climate scenario uncertainties in relation to tolerable regional climate change. *Climate Research*, *10*(1), 1–14.

Huscroft, J., Gleeson, T., Hartmann, J., & Börker, J. (2018). Compiling and Mapping Global Permeability of the Unconsolidated and Consolidated Earth: GLobal HYdrogeology MaPS 2.0 (GLHYMPS 2.0). *Geophysical Research Letters*, *45*(4), 1897–1904. https://doi.org/10.1002/2017GL075860

Ivushkin, K., Bartholomeus, H., Bregt, A. K., Pulatov, A., Kempen, B., & de Sousa, L. (2019).

Global mapping of soil salinity change. *Remote Sensing of Environment*, *231*(December 2018), 111260. https://doi.org/10.1016/j.rse.2019.111260

Kenney, T. A., Gerner, S. J., Buto, S. G., & Spangler, L. E. (2009). *Spatially referenced statistical assessment of dissolved-solids load sources and transport in streams of the Upper Colorado River Basin*. U. S. Geological Survey.

Kim, S., Kim, S., Green, C. H. M., & Jeong, J. (2022). Multivariate polynomial regression modeling of total dissolved-solids in rangeland stormwater runoff in the Colorado River Basin. *Environmental Modelling & Software*, *157*, 105523.

Kittel, T. G. F., Giorgi, F., & Meehl, G. A. (1997). Intercomparsion of regional biases and doubled CO2-sensitivity of coupled atmosphere-ocean general circulation model experiments. *Climate Dynamics*, *14*, 1–15.

Liebermann, T. D., Mueller, D. K., Kircher, J. E., & Choquette, A. F. (1989). *Characteristics and trends of streamflow and dissolved solids in the upper Colorado River Basin, Arizona, Colorado, New Mexico, Utah, and Wyoming*. USGPO; Books and Open-File Reports Section, US Geological Survey [distributor],.

Lindsay, W. L. (1979). *Chemical equilibria in soils.* John Wiley and Sons Ltd.

Liu, W., Park, S., Bailey, R. T., Molina-Navarro, E., Andersen, H. E., Thodsen, H., Nielsen, A., Jeppesen, E., Jensen, J. S., Jensen, J. B., & Trolle, D. (2020). Quantifying the streamflow response to groundwater abstractions for irrigation or drinking water at catchment scale using SWAT and SWAT–MODFLOW. *Environmental Sciences Europe*, *32*(1). https://doi.org/10.1186/s12302-020-00395-6

Lukas, J., Barsugli, J., Doesken, N., Rangwala, I., & Wolter, K. (2014). Climate change in Colorado: a synthesis to support water resources management and adaptation. *University of Colorado, Boulder, Colorado*.

McCarthy, J. J., Canziani, O. F., Leary, N. A., Dokken, D. J., & White, K. S. (2001). *Climate change 2001: impacts, adaptation, and vulnerability: contribution of Working Group II to the third assessment report of the Intergovernmental Panel on Climate Change* (Vol. 2). Cambridge University Press.

Miller, M. P., Buto, S. G., Lambert, P. M., & Rumsey, C. A. (2017). Enhanced and updated spatially referenced statistical assessment of dissolved-solids load sources and transport in streams of the Upper Colorado River Basin. *Scientific Investigations Report*, 34. http://pubs.usgs.gov/sir/2009/5007/%0Ahttp://pubs.er.usgs.gov/publication/sir20175009

Moriasi, D. N., Arnold, J. G., Van Liew, M. W., Bingner, R. L., Harmel, R. D., & Veith, T. L. (2007). Model evaluation guidelines for systematic quantification of accuracy in watershed simulations. *Transactions of the ASABE*, *50*(3), 885–900.

Moriasi, D. N., Gitau, M. W., Pai, N., & Daggupati, P. (2015). Hydrologic and water quality models: Performance measures and evaluation criteria. *Transactions of the ASABE*, *58*(6), 1763–1785.

Mueller, D. K., & Osen, L. L. (1988). *Estimation of natural dissolved-solids discharge in the upper Colorado River basin, western United States* (Vol. 87, Issue 4069). Department of the

Interior, US Geological Survey.

Nauman, T. W., & Duniway, M. C. (2020). A hybrid approach for predictive soil property mapping using conventional soil survey data. *Soil Science Society of America Journal*, *84*(4), 1170–1194.

Nauman, T. W., Ely, C. P., Miller, M. P., & Duniway, M. C. (2019). Salinity Yield Modeling of the Upper Colorado River Basin Using 30-m Resolution Soil Maps and Random Forests. *Water Resources Research*, *55*(6), 4954–4973. https://doi.org/10.1029/2018WR024054

Niswonger, R. G., Panday, S., & Ibaraki, M. (2011). MODFLOW-NWT, a Newton formulation for MODFLOW-2005. *US Geological Survey Techniques and Methods*, *6*(A37), 44.

Olson, J. R. (2019). Predicting combined effects of land use and climate change on river and stream salinity. *Philosophical Transactions of the Royal Society B: Biological Sciences*, *374*(1764). https://doi.org/10.1098/rstb.2018.0005

Park, S. (2018). Enhancement of Coupled Surface/Subsurface Flow Models in Watersheds: Analysis, Model Development Optimization, and User Accessibility. *International Journal of Climatology*, *33*(1), 121–131.

Parkhurst, D. L., & Appelo, C. A. J. (2013). Description of input and examples for PHREEQC version 3—a computer program for speciation, batch-reaction, one-dimensional transport, and inverse geochemical calculations. *US Geological Survey Techniques and Methods*, *6*(A43), 497.

Ragab, R., & Prudhomme, C. (2002). Climate change and water resources management in arid and semi-arid regions: Prospective and challenges for the 21st century. *Biosystems Engineering*, *81*(1), 3–34. https://doi.org/10.1006/bioe.2001.0013

Reclamation, U. S. B. of. (2013). Quality of water, Colorado River Basin—Progress Report No. 24. *US Department of the Interior*, 58.

Rumsey, C. A., Miller, M. P., Schwarz, G. E., Hirsch, R. M., & Susong, D. D. (2017). The role of baseflow in dissolved solids delivery to streams in the Upper Colorado River Basin. *Hydrological Processes*, *31*(26), 4705–4718. https://doi.org/10.1002/hyp.11390

Runkel, R. L., Crawford, C. G., & Cohn, T. A. (2004). *Load Estimator (LOADEST): A FORTRAN program for estimating constituent loads in streams and rivers*.

Santhi, C., Arnold, J. G., Williams, J. R., Dugas, W. A., Srinivasan, R., & Hauck, L. M. (2001). Validation of the swat model on a large rwer basin with point and nonpoint sources 1. *JAWRA Journal of the American Water Resources Association*, *37*(5), 1169–1188.

Schofield, R. V., & Kirkby, M. J. (2003). Application of salinization indicators and initial development of potential global soil salinization scenario under climatic change. *Global Biogeochemical Cycles*, *17*(3), 1–13. https://doi.org/10.1029/2002gb001935

Shangguan, W., Hengl, T., Mendes de Jesus, J., Yuan, H., & Dai, Y. (2017). Mapping the global depth to bedrock for land surface modeling. *Journal of Advances in Modeling Earth Systems*, *9*(1), 65–88.

Shapiro, N. Z., & Shapley, L. S. (1965). Mass action laws and the Gibbs free energy function. *Journal of the Society for Industrial and Applied Mathematics*, *13*(2), 353–375.

Šimůnek, J., Šejna, M., & van Genuchten, M. T. (2012). *The UNSATCHEM Module for HYDRUS (2D/3D) Simulating Two-Dimensional Movement of and Reactions Between Major Ions in Soils*. Version.

Smith, I., & Chandler, E. (2010). Refining rainfall projections for the Murray Darling Basin of south-east Australia—the effect of sampling model results based on performance. *Climatic Change*, *102*(3–4), 377–393.

Smith, L. A. (2002). What might we learn from climate forecasts? *Proceedings of the National Academy of Sciences*, *99*(suppl_1), 2487–2492.

Spahr, N. E., Apodaca, L. E., Deacon, J. R., Bails, J. B., Bauch, N. J., Smith, C. M., & Driver, N. E. (2000). *Water quality in the upper colorado river basin, colorado, 1996-98* (Issue 1214). US Geological Survey.

Stainforth, D. A., Allen, M. R., Tredger, E. R., & Smith, L. A. (2007). Confidence, uncertainty and decision-support relevance in climate predictions. *Philosophical Transactions of the Royal Society A: Mathematical, Physical and Engineering Sciences*, *365*(1857), 2145–2161.

Tavakoli-Kivi, S., Bailey, R. T., & Gates, T. K. (2019). A salinity reactive transport and equilibrium chemistry model for regional-scale agricultural groundwater systems. *Journal of Hydrology*, *572*(December 2018), 274–293. https://doi.org/10.1016/j.jhydrol.2019.02.040

Tillman, F. D., & Anning, D. W. (2014). A data reconnaissance on the effect of suspended-sediment concentrations on dissolved-solids concentrations in rivers and tributaries in the Upper Colorado River Basin. *Journal of Hydrology*, *519*(PA), 1020–1030. https://doi.org/10.1016/j.jhydrol.2014.08.020

Tillman, F. D., Anning, D. W., Heilman, J. A., Buto, S. G., & Miller, M. P. (2018). Managing salinity in upper Colorado River Basin streams: Selecting catchments for sediment control efforts using watershed characteristics and random forests models. *Water (Switzerland)*, *10*(6), 1–17. https://doi.org/10.3390/w10060676

Tirabadi, M. S. M., Banihabib, M. E., & Randhir, T. O. (2021). SWAT-S: A SWAT-salinity module for watershed-scale modeling of natural salinity. *Environmental Modelling & Software*, *135*, 104906.

Tuteja, N. K., Beale, G., Dawes, W., Vaze, J., Murphy, B., Barnett, P., Rancic, A., Evans, R., Geeves, G., & Rassam, D. W. (2003). Predicting the effects of landuse change on water and salt balance—a case study of a catchment affected by dryland salinity in NSW, Australia. *Journal of Hydrology*, *283*(1–4), 67–90.

Vengosh, A. (2014). 11.9 - Salinization and Saline Environments. In H. D. Holland & K. K. Turekian (Eds.), *Treatise on Geochemistry (Second Edition)* (Second Edi, pp. 325–378). Elsevier. https://doi.org/https://doi.org/10.1016/B978-0-08-095975-7.00909-8

Warner, J. W., Heimes, F. J., & Middelburg, R. F. (1985). *Ground-water contribution to the salinity of the upper Colorado River Basin* (Vol. 84, Issue 4198). US Department of the Interior, Geological Survey.

Weltz, M. A., Nouwakpo, S. K., Rossi, C., Jolley, L. W., & Frasier, G. (2014). *Salinity Mobilization and Transport from Rangelands: Assessment, Recommendations, and Knowledge Gaps*. *April*, 72. http://www.coloradoriversalinity.org/docs/Salinity Mobilization and Transport from Rangelands.pdf

White, M. J., Gambone, M., Haney, E., Arnold, J., & Gao, J. (2017). Development of a station based climate database for SWAT and APEX assessments in the US. *Water (Switzerland)*, *9*(6), 1–9. https://doi.org/10.3390/w9060437

Williams, J. R., & Izaurralde, R. C. (2010). The APEX model. In *Watershed models* (pp. 461–506). CRC Press.

Williams, W. D. (1999). Salinisation: A major threat to water resources in the arid and semi-arid regions of the world. *Lakes and Reservoirs: Research and Management*, *4*(3–4), 85–91. https://doi.org/10.1046/j.1440-1770.1999.00089.x

Worqlul, A. W., Jeong, J., Green, C. H. M., & Abitew, T. A. (2021). The impact of rainfall distribution methods on streamflow throughout multiple elevations in the Rocky Mountains using the APEX model—Price River watershed, Utah. *Journal of Environmental Quality*, *50*(6), 1395–1407. https://doi.org/10.1002/jeq2.20298

Zaman, M., Shahid, S. A., & Heng, L. (2018). Introduction to Soil Salinity, Sodicity and Diagnostics Techniques. In *Guideline for Salinity Assessment, Mitigation and Adaptation Using Nuclear and Related Techniques*. https://doi.org/10.1007/978-3-319-96190-3_1

Zhang, J., Lu, C., Crumpton, W., Jones, C., Tian, H., Villarini, G., Schilling, K., & Green, D. (2022). Heavy Precipitation Impacts on Nitrogen Loading to the Gulf of Mexico in the 21st Century: Model Projections Under Future Climate Scenarios. *Earth's Future*, *10*(4), 1–17. https://doi.org/10.1029/2021EF002141

Zhulu, L. (2010). Getting Started with PEST. *Athens, The University of Georgia*.

APPENDIX A

Table 7- APEX model Parameter used for PEST Calibration.

Name	Lower Range	Upper Range	Initial value	Description
p005	0	1	0.5	Soil water lower limit (Range is from 0 - 1) lower limit of water content in the top 0.5 m soil depth expressed as a fraction of the wilting point water content. (cols. 33-40)
p012	1.5	2.5	2.5	Soil evaporation coefficient, (Range is from 1.5 - 2.5), governs rate of soil evaporation from top 0.2 m of soil.
p015	0	0.3	0	Runoff CN Residue Adjustment Parameter (Range is from 0.0 - 0.3). Increases runoff for RSD < 1.0 t/ha; Decreases for RSD > 1.0 t/ha.
p016	1	1.5	1	Expands CN retention parameter (Range is from 1.0 - 1.5). Values > 1.0 expand CN retention and reduce runoff.
p017	0	0.5	0.25	Soil evaporation – plant cover factor (Range is from 0.00 - 0.5). Reduces effect of plant cover as related to LAI in regulating soil evaporation.
p020	0.05	0.4	0.2	Runoff curve number initial abstraction (Range is from 0.05 - 0.4)
p023	0.0023	0.0032	0.0032	Hargreaves PET equation coefficient (Range is from 0.0023 - 0.0032), original value = 0.0023, current value = 0.0032
p025	0	2	0	Exponential coefficient used to account for rainfall intensity on curve number
p034	0.5	0.6	0.5	Hargreaves PET equation exponent (Range is from 0.5 - 0.6) original value=0.5. Modified to 0.6 to increase PET.
p040	0.001	1	1	Groundwater storage threshold (Range is from 0.001 - 1.) fraction of groundwater storage that initiates return flow. Return flow will not occur unless the fraction of maximum groundwater storage > Parm 40.
p042	0.3	2.5	1	SCS curve number index coefficient (Range is from 0.3 -2.5) regulates the effect of PET in driving the SCS curve number retention parameter.
p044	1	2	1.2	Upper Limit of Curve Number Retention Parameter S (Range is from 1.0 - 2.0) SUL=PARM (44)*S1. Allows CN to go below CN1.
p049	0	15	7	Maximum rainfall interception by plant canopy (mm) (Range is from 0.0 - 15.0)
p050	0.05	0.3	0.1	Rainfall interception coefficient, (Range is from 0.05 - 0.3)
p051	0.1	0.9	0.5	Water stored in litter (residue) coefficient (Range is from 0.1 - 0.9). Fraction of litter weight.
p061	0.05	0.95	0.2	Soil water Upward Flow Limit (Range is from 0.05 – 0.95) Limits water tension ratio used to move water from a lower layer to the one above it.
ap089	0.1	0.9	0.1	Water table recession exponent (Range is from 0.1 – 0.9) Exponent of day of year/365
p090	1	100	2	Subsurface flow factor (Range is from 1.0 – 100.0) Traditional value is 2.0.
p091	0.001	1	0.1	Flood Evaporation Limit (Range is from 0.001 – 1) Allows for limiting of evaporation of flood waters during flooding. Regulates evaporation from channel and floodplain.
p092	0.1	2	1	Runoff Volume Adjustment for Direct Link (NVCN = 0) (Range is from 0.1 to 2.0) Inversely related to runoff. Used like Parm 42 in CN index method (NVCN = 4).
p095	0	15	7	(Testing: melting point) Exponent of Crop Stress Temperature function (Range is from 0.8 – 2.0). Setting this parameter to 1 causes no effect.

APPENDIX B

Table 8- The following regression equations were used in the LOADEST calculations of daily ion loads. LOADEST automatically select the best fit regression equation for each ion with the measured data.

Salt Ion	**Regression Equation**	**AMLE R^2 (%)**	**BP (%)**	**NSE**
HCO_3^-	$\ln(Load) = 13.2517 + (0.9579\ln(Q))$	30.12	-6.65	0.45
Ca^{2+}	$\ln(Load) = 11.8005 + (0.9227\ln(Q)) + (0.3338Sin(2pidtime)) + (-0.0970Cos(2pidtime)) + (-0.0474dtime)$	63.06	-2.77	0.74
Mg^{2+}	$\ln(Load) = 11.5624 + (0.3867\ln(Q)) + (0.0794Sin(2pidtime)) + (0.0715Cos(2pidtime))$	66.35	-0.12	0.76
Na^+	$\ln(Load) = 10.2489 + (1.3305\ln(Q)) + (0.5933Sin(2pidtime)) + (-0.1675Cos(2pidtime)) + (-0.1053dtime)$	42.39	-5.11	0.38
Cl^-	$\ln(Load) = 12.3355 + (-0.1392\ln(Q))$	0.48	52.23	-0.89
K^+	$\ln(Load) = 9.6980 + (0.4141\ln(Q)) + (0.1064\ln(Q^2))$	57.66	0.22	0.81
SO_4^{2-}	$\ln(Load) = 13.6361 + (0.5186\ln(Q))$	63.36	-3.27	0.47

APPENDIX C

Table 9- The NOAA climate station at Crested Butte, CO, US measured monthly precipitation against 20 available CMIP 5 GCMs precipitation performance results for RCP 4.5 are shown. GCMs are ranked based on total ranking score.

GCM	**Mean R.E (mm)**	**Std R. E**	**NRMSE**	**Corr (Mon Dis)**	**Kendal Slope (mm/year)**	***Brier score***	***S score***	**Total Ranking Score**
NOAA					-0.982			
bcc-csm1-1(China)	0.10	0.08	1.31	0.08	-1.065	4.99E-05	77	26.41
bcc-csm1-1-m (China)	0.09	0.12	1.30	0.07	0.538	5.26E-05	78	29.00
BNU-ESM (China)	0.10	0.05	1.26	0.18	1.126	6.45E-05	73	31.04
CanESM2 (Canada)	0.05	0.17	1.28	0.05	-3.349	6.48E-05	77	21.31
CCSM4 (USA)	0.08	0.08	1.26	0.15	1.273	3.63E-05	81	30.12
CNRM-CM5 (France)	0.11	0.21	1.24	0.09	0.708	5.81E-05	78	33.04
CSIRO-Mk3-6-0 (Australia)	0.04	0.09	1.31	0.07	-0.272	6.54E-05	75	23.50
GFDL-ESM2M (USA)	0.09	0.09	1.28	0.12	2.051	5.32E-05	75	30.16
GFDL-ESM2G (USA)	0.12	0.13	1.35	-0.01	1.154	5.65E-05	75	29.62
HadGEM2-CC365 (United Kingdom)	0.05	0.03	1.30	0.09	-0.620	6.97E-05	73	21.79
HadGEM2-ES365 (United Kingdom)	0.10	0.14	1.30	0.05	2.190	4.75E-05	77	30.82
inmcm4 (Russia)	0.06	0.17	1.27	0.06	-0.304	7.17E-05	73	25.17
IPSL-CM5A-LR (France)	0.07	0.03	1.28	0.16	0.799	5.07E-05	77	27.24
IPSL-CM5A-MR (France)	0.12	0.06	1.34	0.06	2.842	5.09E-05	77	33.22
IPSL-CM5B-LR (France)	0.04	-0.05	1.45	0.00	-0.434	4.80E-05	79	20.83
MIROC5 (Japan)	0.06	-0.01	1.39	0.04	1.665	4.40E-05	79	25.63
MIROC-ESM (Japan)	0.12	0.00	1.36	0.09	2.123	4.81E-05	79	33.53
MIROC-ESM-CHEM (Japan)	0.01	-0.05	1.41	0.05	-0.620	3.39E-05	81	18.42
MRI-CGCM3 (Japan)	0.05	-0.04	1.45	-0.01	-0.041	4.39E-05	80	22.16
NorESM1-M (Norway)	0.07	0.00	1.37	0.06	-0.113	5.47E-05	75	23.48